Paleomagnetic implications on the stability of the Moesian Platform and the Bulgarian Rhodope since the Paleogene: surviving in between two major rotating systems

Karen Oud
MSc Geology student, Faculty of Geosciences, Utrecht University
July 2008

Abstract

To investigate whether or not the Moesian Platform and the Bulgarian Rhodope accommodated for the major clockwise rotation of both the Carpathian and Aegean systems since 13 Ma, paleomagnetic analysis was done on Paleogene sediments and volcanics from the Moesian Platform and volcanics from the Bulgarian Rhodope. The mean paleomagnetic direction for the overall Bulgarian region shows a declination of $11^o \pm 10^o$ N at 30 Ma. Hence, with respect to the overall rotation of the Eurasian continent, the Bulgarian region is a stable block with a negligible rotation of $4.3^o \pm 10.9^o$ counterclockwise since 30 Ma.

1. Introduction

The Moesian Platform in northern Bulgaria lies in between two domains that have shown a clear rotation since the Middle Miocene, which is proven in several studies. The southern Carpathian foreland in Romania, north of the Moesian Platform, rotated from 13 to 8 Ma by 30^o clockwise (CW) (Dupont-Nivet et al, 2005). During the same period, the Greek Rhodope massif in the northeast of the Aegean region underwent a rotation of 20^o to 30^o CW (Van Hinsbergen et al, 2005). Both mountain belts formed during the Alpine orogeny in the Tertiary. They are joined together south (with the Balkanides, see figure 1) and west of the Moesian platform (Schmid et al, 1998).

Not much is known yet about the rotational evolution of the Moesian Platform and the Bulgarian Rhodope during the Alpine orogeny. Moreover, previous studies that have dealt with these areas do not give a decisive outcome of the results. Jordanova et al (2001) cite some contrasting results from different studies concerning northern Bulgaria: the Moesian platform would have rotated counterclockwise (CCW), or, it underwent hardly any rotation. Also, it is long believed that the Moesian platform is a stable domain in between the two tectonically active systems. Schmid et al (1998) state that during the Late Cretaceous, the western part of the Rhodope moved northwards, past the Moesian Platform. They also state that the stable Moesian Platform served as a corner, around which oroclinal bending (arc formation) of the Southern Carpathians occurred during the Eocene. This bending would cause major dextral wrenching and clockwise rotations in the Southern Carpathian units relative to the Moesian Platform.

However, because the Carpathian and Aegean domains underwent such a major rotation, it is very well possible and it may seem logical that the Moesian platform accommodated for this movement with a similar rotation itself.

The goal of this study is to investigate whether or not the Moesian platform and the Bulgarian Rhodope indeed underwent such a rotation since at least 13 Ma, and if so, how much this rotation was exactly. For this, extensive paleomagnetic sampling was done on the Moesian Platform and in the Bulgarian Rhodope, from both late Cretaceous to Miocene sediments and Oligocene volcanic plugs; the latter mostly in the Rhodope volcanic massif. Also, some rock magnetic experiments were carried out to determine the dominant ferromagnetic minerals in the different localities.

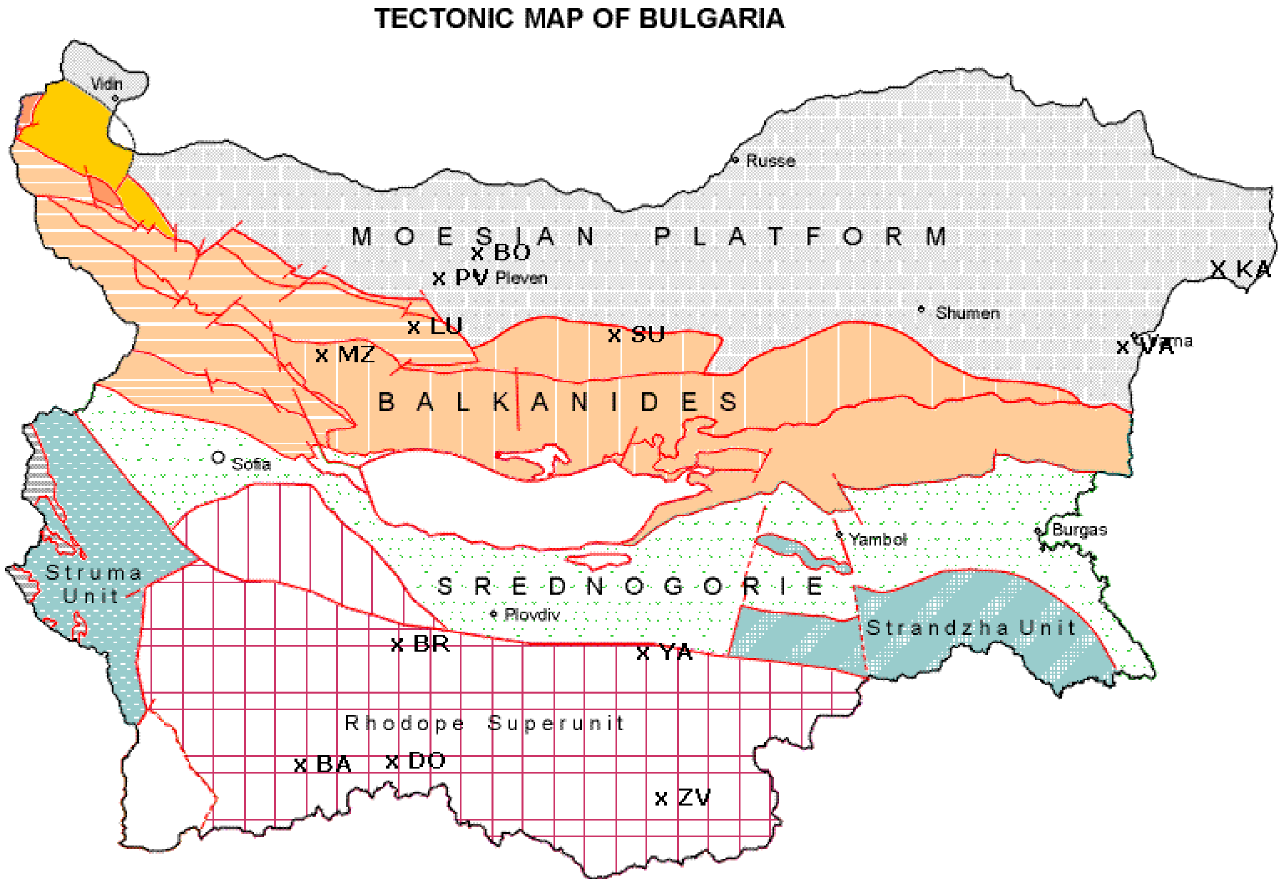

Figure 1*. Map of the main tectonic zones in Bulgaria with sampling localities. Moesian Platform: stable part, mainly Neogene-Quaternary sedimentary cover; Balkanides: low degree of Alpine deformation, mainly Cretaceous-Paleogene cover; Srednogorie: volcanic (island arc) basement, folded and thrusted northward during Late Cretaceous; Rhodope unit: Alpine metamorphic complex formed from Paleozoic-Mesozoic crustal and mantle fragments with Paleogene sedimentary and volcanic cover. Sedimentary localities: BO – Bojouritsa; PV – Pleven; LU – Lukovit; MZ – Mezdra; VA – Varna; KA – Kavarna. Volcanic localities: SU – Suhindol; BR – Bratsigovo; YA – Yabalkovo; ZV – Zvesdel; DO – Dospat; BA – Banichan. After Georgiev et al (2000).*

2. Geological setting and sampling

2.1. Sites

Sampling was done at twelve localities from a large area covering the Moesian Platform and the Bulgarian Rhodope (see figure 1). At each locality, around 7 to 12 sites (with exceptions of Mexdra and Banichan, having 20 and 4 sites, respectively) were drilled, which were spread out over several outcrops to average possible local rotations and include as much time as possible. Each site consisted generally of 8 samples, resulting in a total number of 960 samples.

On the Moesian Platform, upper Cretaceous and younger sediments were sampled, as well as a volcanic complex with basaltic plugs intruding the sediments. This was done to enhance chances of results, because the sediments were mainly marine carbonates (limestones and mudstones), which do not always have a high chance of preserving the paleomagnetic signal. For the same reason, the volcanic sites in the Rhodope were sampled.

Moesian sediments were sampled at six localities, with ages ranging from upper Cretaceous-Paleocene (in Mezdra and Bojouritsa localities) to Eocene (in Pleven and Varna localities), and even younger sediments having Miocene age (in Lukovit and Kavarna localities). All sediments are not, or only, slightly tilted. Bedding dips range from a maximum of 17^{o} for some samples from the Paleocene, to $<5\text{-}7^{o}$ dip for samples from the Miocene. Paleomagnetic directions resulting from the demagnetizations were corrected for this bedding-tilt.

A series of three basaltic plugs was sampled on a locality near Suhindol, in the Moesian Platform. These basalts have been radiochronologically dated to be of early Miocene age, ranging from 20 to 25 Ma.

In the Rhodope of southern Bulgaria, volcanics were sampled at five localities. They have been radiochronologically dated at 25 to 35 Ma. From the same age range, localities have been sampled (1) in the eastern Rhodope including lavas near Yabalkovo and basaltic to andesitic lavas near Zvezdel, and (2) in the western Rhodope. Those are all felsic extrusives varying from rhyolitic lavas to ignimbrites (Bratsigovo, Dospat and Banichan).

2.2. Sampling

Sampling was done with a portable drill powered with gasoline. Drill bits with diamond coating were cooled with water from a pump. Cores from such a drill are about 2.5 cm in diameter and they must have a minimum length of about 6 cm to be useful for getting multiple samples from each core. The orientation of the sample was measured with a magnetic compass. A correction of 4^{o} for local declination in Bulgaria was taken into account for all measurements. Orientation and identification marks were put on the sample before it was wrapped in aluminium foil for optimal preservation. At every site, GPS-points were taken for precise location. In case of a visible bedding (in sampled sediments, or surrounding a sampled volcanic horizon), the strike and dip were measured.

Some remarks can be made on the sampling methods above. It is important that samples are taken from seemingly fresh, non-weathered rocks. Weathering can alter the paleomagnetic signal in a way that it is weakened and is overprinted by the present-day magnetic signal through oxidation of primary magnetite or hematite. Thus, it was necessary to be careful on choosing fresh sites, like road cuts, or creating fresh outcrop by digging into sediments and removing the outer layer. Furthermore, at outcrops with loose blocks much care must be taken on drilling samples in a fixed block, because otherwise, orientations could have been false.

For sediments, another measure was also taken into account. Sedimentation occurs relatively slowly compared to cooling of lava flows and igneous intrusions and therefore, sediment layers can cover a large time range. It is important to try and take samples from one site as much as possible in the same sedimentary layer to diminish effect of the observed variation in the paleomagnetic field through time.

3. Paleomagnetic analysis

3.1. Demagnetization

The magnetic signal preserved in rocks, before treatment, is the natural remanent magnetization (NRM). This NRM often consists of multiple components; a primary component that originated during rock formation, and a secondary component that was acquired at later times by other processes, either gradual or short-term. The latter can alter the first component and adds up to the total NRM. However, because in most studies the primary is needed, the secondary NRM must be disposed off from the sample. Fortunately, this is, in most cases, the less stable component. Partial demagnetization can remove it from the sample and will isolate the more stable component. The latter is then called the characteristic NRM (ChRM), because it is not fully certain whether this is only the primary NRM.

All the samples were treated at the paleomagnetic lab of Fort Hoofddijk in Utrecht. The NRM of all samples was measured in a 2G Enterprises horizontal DC-SQUID cryogenic magnetometer, which is able to handle samples that are only weakly magnetized. Inside, the multiple components (M_x, M_y, M_z) of the magnetic moment of the sample are measured in different positions. The orientation data are then compared with known orientation for the sample and the bedding attitude, and the resulting geographic and stratigraphic directions of the NRM are calculated.

From each sampling site, one sample was measured in a first round, from both the sediments and the volcanics. The goal of this round was to investigate which sites had a strong and sensible magnetic signal and which ones would have no or hardly any good signal. For this first round, samples were thermally demagnetized. A piece of about 2.5 cm thick was sawn from the samples. These were heated in several stages in a magnetically shielded oven, with temperatures starting at room temperature (20^{o}C), followed by two steps of 80^{o}C and steps of 30^o after that, to a maximum of 360^{o}C. Thermal demagnetization results in a stepwise removal of the secondary NRM from all grains that have a blocking temperature below the demagnetization temperature.

Most of the samples were at least heated to 180^{o}C or 210^{o}C, however, when the result at that stage did not make any sense anyhow, the sample would be rejected from further analysis. Other samples were rejected at later stages because those also gave useless, non-interpretable results and/or because most samples from that site were already rejected earlier. From sediment samples with a reasonable or good signal, the rest of the site was prepared and measured in the DC-SQUID by the same procedure.

All of the volcanics were demagnetized by applying an alternating field (AF). The AF demagnetizer is situated in a magnetically shielded room and is aided by a robot-navigated device which handles the samples. In the AF demagnetizer, the samples are exposed to an alternating field which decreases with time and destroys the secondary NRM with less coercivity than the original applied pick field. The demagnetization was done with pick field steps of 5 mT, starting from 0 mT and with steps of 10 mT, from 30 mT on, to a maximum pick field of 100 mT.

3.2. Rock magnetic experiments

Generally, rock magnetic experiments on samples are run to determine the magnetic minerals in samples and to investigate whether a measured NRM is primary or secondary. For this study, the variation in low-field magnetic susceptibility was tested for one sample from each volcanic locality.

About 200 mg from each sample was crushed. The susceptibility of the powder was measured during heating and cooling using a KLY3-CS Kappabridge susceptibility meter. This was done in two cycles: 40-400-40^{o}C and 40-700-40^{o}C. The resulting diagram gives the variation in susceptibility, from which the Curie temperature can be determined and, consequently, indications on the magnetic mineral involved. Curie temperatures are the points of major decrease in susceptibility and vary from one magnetic mineral to the other.

3.3. ChRM directions

All demagnetization diagrams were analysed with the laboratory software Paldir, Palfit and Pal_vD_s, the latter for the site mean directions and confidence level. Palfit calculates site and locality mean directions for greatcircles, which determine the direction of the most stable component. In the case of a measured (surrounding) bedding-tilt, the Paldir program corrected the measured direction for this tilt. For all sites, κ and α95 values were calculated. Those values give a grading for the confidence level of the results: 'good' results are designated by a κ of >30 and a α95 of <15°. This confidence level is a measure of how much scatter or deviation from the mean is present in a site. Sites that had lower or higher values, respectively, were rejected from further calculations. For lavas, those values are an expression of the measuring error only, because lavas cool relatively quickly and are therefore unable to incorporate any secular variation. For sites is considered that measuring errors are averaged out. For locality means the observed scatter is thus not caused by measuring errors anymore, but represents spot readings of secular variation recorded by each separate lava.

For all volcanic sites and localities, average paleo-pole positions were determined with Palpole. These are represented by λ (latitude of the pole), φ (longitude of the pole), paleo-colatitude (palat) and K and A95, which are again measures of the confidence level. This paleopole determination is important for averaging out effects of secular variation, causing the declination and inclination of the magnetic field to vary for different locations at different times. The position of the overall magnetic pole is independent of those variations. By knowing the pole position at a certain time in the past, it can be investigated whether the observed change in magnetic direction (compared to the expected paleomagnetic direction at that time) is only local, caused by a local rotation of minor importance, or whether it is observed over a much larger area (tectonic scale). With A95 and palat, the deviation in declination (ΔD) and inclination (ΔI) were calculated for every separate locality and overall. Scatter in pole positions is caused by secular variation, therefore, K and A95 are only provided on the tables for localities and not for individual lavas (sites).

A last step was done by comparing the direction of the magnetic field and position of the reference magnetic for Eurasia at 30 Ma (Torsvik et al, 2008 - in press) with the mean direction and position that was calculated for all volcanic sites. The result of this calculation tells whether there has been, in the observed area, a rotation with respect to the Eurasian continent since 30 Ma.

Locality	***Location***		***Age***		***Direction***					
	Lat	*Lon*		*Tilt*	*Dec*	*Inc*	*κ*	*α95*	*Na*	*Ng*
Lukovit			***Miocene***		***8.5***	***44.9***			***7***	***0***
LU 1	43.1131	24.1063		324/07	37.3	50.5	319.8	5.1	8	4
LU 2	43.1131	24.1063		324/07	8.7	-41.4	2509.6	1.8	8	4
LU 3	43.1131	24.1063		324/07	9.1	-7.8	3100.1	2.2	8	3
LU 4	43.1184	24.1067		324/07	38.7	5.4	576.7	2.5	8	7
LU 5	43.1184	24.1067		349/06	53.6	12.8	0.0	99.9	8	2
LU 6	43.1184	24.1067		349/06	58.7	51.5	81.3	7.5	8	6
LU 7	43.1184	24.1067		349/06	136.2	-28.6	0.0	99.9	8	2
Mezdra			***Up. Cretaceous/ Paleocene***							
MZ 2	43.0838	23.4294		298/06	185.7	-57.8	131.0	4.9	8	8
MZ 15	43.1318	23.4009		091/12	317.2	-0.7	39.8	14.7	8	4

Table 1*. AF demagnetization results for sampled sediments with a promising signal after first thermal demagnetization. Na = number of analysed samples/sites; Ng = number of used 'good' samples/sites.*

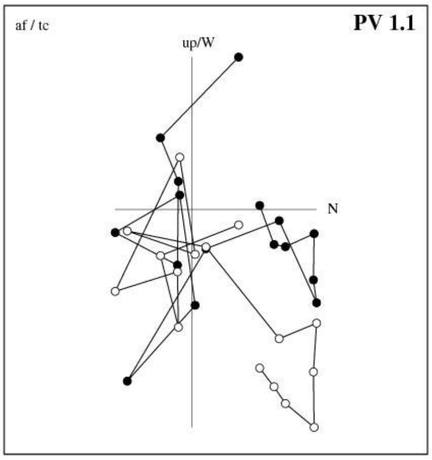

***Figure 2a**. An example of a complicated multi-component sample (PV 1.1) that was rejected from further investigation.*

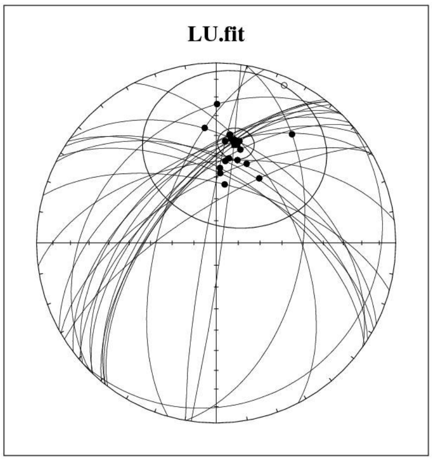

***Figure 2b**. Equal area plot of the mean locality direction for Lukovit, calculated with greatcircles.*

4. Results

4.1. Sediments

In general, the sediment samples gave quite bad results. Many of them were complicated multi-component samples with a high influence from overprinting, figure 2a shows a typical example. In other samples, it was possible that transformation of magnetic minerals during heating caused a new magnetic signal to come up.

Only the samples from the Lukovit locality (Miocene mudstones), and two sites from the Mezdra locality (Paleocene limestones) had a quite useful signal after AF demagnetization. The resulting Paldir plots from LU were mostly greatcircles. The mean direction for the whole locality, as calculated with Palfit, is shown in figure 2b. The mean results per site are shown in table 1, as well as the site mean direction calculated from the greatcircles.

As can be seen, not all sites give results that are as acceptable as others. LU5 and LU7 with only 2 samples each are definite outliers; according to their κ and α95 values they are useless. Furthermore, LU2 and LU3 have surprisingly high κ values, which are probably not reliable. Even for very high quality volcanics, it is uncommon to have such high κ values. The last column of the table shows that in general, the number of reliable samples is low.

Most of the magnetic signals in the Lukovit samples have a normal polarity (designated by a vector pointing northward and 'down' or positive for the Northern Hemisphere). The sites from Mezdra show a mostly reversed polarity (thus southward and 'up' or negative).

Because the number of reliable samples and sites is too low to generate a meaningful result, no paleopole is calculated for the sediments. Therefore, they will not be taken into account for the overall conclusion of this study.

3.2. Volcanics

As expected, the results for the volcanic localities are much better. Most of the sites from each locality have been proven useful after AF demagnetization. This is shown by good κ and α95 values of several hundreds and well below 15^{o} respectively, which are typical values for an average 'good' volcanic site. All results are shown in table 2. As with the sediments, some outliers exist in all localities; however, most of them are not as extreme.

Most individual diagrams show a path towards the origin along a clear vector line during evolving demagnetization, which is the perfect implication of a degenerating characteristic NRM. As can be seen in table 2, almost all sites have a reversed paleomagnetic signal; only a few sites from Suhindol show a normal polarity. Example plots from Suhindol are given in figure 3a and b. As can be seen, there are only seven out of twelve sites used from Suhindol. This is unfortunately caused by an unrecoverable error in the output file from the magnetometer.

Overprint by another, secondary magnetic component can be seen clearly

Locality (1)	***Location***		***Age***		***Pole***					***Direction***							
	Lat	*Lon*		*Tilt*	*λ*	*φ*	*K*	*A95*	*palat*	*Dec*	*ΔD*	*Inc*	*ΔI*	*κ*	*α95*	*Na*	*Ng*
Overall mean	***41.5***	***25.3***			***81.2***	***96.1***	***11.7***	***7.5***	***43.9***	***191.6***	***10.4***	***-62.5***	***6.1***	***-***	***-***		
Reference pole	***41.56***	***25.33***			***82.7***	***152.1***	***-***	***2.8***	***36.9***	***187.3***	***3.5***	***-56.4***	***2.7***	***-***	***-***		
Suhindol			***20-25 Ma***		***74.2***	***63.7***	***6.0***	***40.8***	***54.5***	***200.8***	***?[1)]***	***-67.9***	***29.1***	***-***	***-***	***12***	***4***
SU 1	43.1681	25.1263		-	-	-	-	-	-	49.3	-	-46.1	-	3.1	37.8	8	8
SU 2	43.1681	25.1263		-	44.3	100.3	-	-	37.7	240.9	-	-56.9	-	507.3	2.5	8	8
SU 3	43.1681	25.1263		-	-	-	-	-	-	71.6	-	-18.1	-	12.4	16.4	8	8
SU 5	43.2902	25.1736		-	66.7	155.0	-	-	26.4	20.0	-	44.5	-	118.9	5.6	8	7
SU 6	43.2902	25.1736		-	-	-	-	-	-	341.0	-	23.4	-	3.3	36.4	8	8
SU 7	43.2902	25.1736		-	54.7	356.1	-	-	68	311.4	-	78.5	-	118.1	5.1	8	8
SU 12	43.2285	25.1526		-	69.9	4.3	-	-	61.3	345.2	-	74.6	-	397.9	2.8	8	8
Yabalkovo			***25-35 Ma***		***72.3***	***26.0***	***34.9***	***8.3***	***59.7***	***180.2***	***16.6***	***-73.3***	***5.2***	***-***	***-***	***12***	***10***
YA 1	42.0415	25.2345		-	50.1	42.5	-	-	75.6	228.7	-	-82.5	-	117.9	5.1	8	8
YA 2	42.0415	25.2345		-	-	-	-	-	-	94.1	-	-50.5	-	1.5	75.9	8	8
YA 3	42.0415	25.2345		-	78.3	25.8	-	-	53.7	180.1	-	-69.8	-	457.5	2.6	8	8
YA 4	42.0415	25.2345		-	62.2	33.5	-	-	69.3	191.3	-	-78.9	-	63.2	7.0	8	8
YA 5	42.0446	25.2450		254/05	-	-	-	-	-	25.0	-	-14.8	-	3.2	37.2	8	8
YA 6	42.0446	25.2450		254/05	70.8	359.2	-	-	58.4	164.1	-	-72.8	-	259.2	4.2	8	6
YA 7	42.0446	25.2450		254/05	56.4	17.5	-	-	74.8	163.4	-	-82.3	-	1445.2	1.6	8	7
YA 8	42.0446	25.2450		254/05	73.5	337.6	-	-	51.6	160.2	-	-68.3	-	412.2	2.7	8	8
YA 9	42.0346	25.2773		-	70.0	32.5	-	-	61.8	185.2	-	-74.9	-	241.3	3.6	8	8
YA 10	42.0346	25.2773		-	82.4	242.2	-	-	35.8	175.0	-	-63.3	-	68.8	6.7	8	8
YA 11	42.0346	25.2773		-	78.3	52.3	-	-	52.2	187.9	-	-68.1	-	65.2	6.9	8	8
YA 12	42.0346	25.2773		-	79.1	74.1	-	-	48.6	191.9	-	-66.1	-	128.6	4.9	8	8
Zvesdel			***25-35 Ma***		***73.9***	***119.3***	***15.3***	***17.7***	***38.2***	***200.7***	***22.8***	***-55.6***	***17.3***	***-***	***-***	***12***	***6***
ZV 1	41.2781	25.2499		-	72.7	158.9	64.4	6.5	28.4	194.6	-	-45.9	-	73.4	6.5	8	8
ZV 2	41.2745	25.2493		-	-	-	-	-	-	39.7	-	-26.5	-	10.0	18.4	8	8
ZV 4	41.2712	25.2478		-	-	-	-	-	-	188.9	-	-48.7	-	20.7	12.5	8	8
ZV 5	41.2656	25.2511		-	-	-	-	-	-	63.0	-	-13.8	-	8.3	20.5	8	8
ZV 6	41.2651	25.2509		-	72.3	180.0	-	-	24.9	188.2	-	-42.9	-	249.8	3.8	8	7
ZV 8	41.2539	25.2561		-	63.1	88.3	-	-	47.9	216.8	-	-65.5	-	212.4	4.2	8	7
ZV 9	41.2471	25.2567		-	70.8	146.9	-	-	29.5	199.2	-	-48.4	-	74.9	7.0	8	7
ZV 10	41.2469	25.2480		-	53.0	117.4	-	-	30.6	224.1	-	-49.3	-	88.5	6.5	8	7
ZV 12	41.2444	25.2466		324/15	65.9	13.9	-	-	64.5	169.9	-	-76.3	-	87.8	6.5	8	7

Locality (2)	***Location***		***Age***	***Pole***					***Direction***							
	Lat	*Lon*	*Tilt*	*λ*	*φ*	*K*	*A95*	*palat*	*Dec*	*ΔD*	*Inc*	*ΔI*	*κ*	*α95*	*Na*	*Ng*
Bratsigovo			***25-35 Ma***	***-3.1***	***64.5***	***1.6***	***99.9***	***32***	***313.1***	***?***[1)]	***-49.2***	***113.9***	***-***	***-***	***4***	***3***
BR 1	42.0175	24.2601	224/20	-26	37.7	-	-	20.9	347.0	-	-37.6	-	388.9	3.4	8	7
BR 2	42.0173	24.2603	244/12	59.9	142.1	-	-	23.9	208.9	-	-41.5	-	201.1	3.9	8	8
BR 3	42.0173	24.2603	244/12	-31.4	36.8	-	-	15.7	348.6	-	-28.8	-	356.2	3.6	8	6
BR 4	42.0169	24.2604	244/12	-	-	-	-	-	56.1	-	-41.8	-	2.0	53.1	8	8
Dosbat			***25-35 Ma***	***67.4***	***136.4***	***102.4***	***5.1***	***29.8***	***204.4***	***5.9***	***-48.8***	***5.9***	***-***	***-***	***10***	***9***
DO 1	41.4102	24.0940	-	71.9	118.7	-	-	37.6	201.7	-	-57.5	-	189.0	4.4	8	7
DO 2	41.4102	24.0940	-	60.0	136.4	-	-	25.5	210.8	-	-43.5	-	222.6	4.1	8	7
DO 3	41.4103	24.0922	-	68.4	127.6	-	-	33.4	204.6	-	-52.8	-	419.8	2.7	8	8
DO 4	41.4104	24.0919	-	61.6	128.1	-	-	29.7	211.9	-	-48.5	-	176.0	4.2	8	8
DO 5	41.4111	24.0917	-	68.1	138.8	-	-	29.8	203.1	-	-48.6	-	190.1	4.0	8	8
DO 6	41.4111	24.0917	-	63.6	150.0	-	-	23.4	203.1	-	-40.8	-	333.7	3.0	8	8
DO 7	41.4131	24.0920	-	75.0	116.1	-	-	39.2	199.2	-	-58.0	-	106.8	5.4	8	8
DO 8	41.4130	24.0912	-	75.0	173.6	-	-	28.1	192.0	-	-47.1	-	103.0	5.5	8	8
DO 9	41.4135	24.0878	-	58.8	139.4	-	-	23.6	210.6	-	-40.8	-	154.7	4.5	8	8
Banichan			***25-35 Ma***	***65.3***	***277.2***	***29.6***	***17.2***	***30.9***	***152.5***	***20.2***	***-49.8***	***19.3***	***-***	***-***	***8***	***4***
BA 2	41.3857	23.4211	-	52.3	280.1	-	-	24.7	140.5	-	-47.3	-	326.5	3.7	8	6
BA 3	41.3854	23.4218	-	-	-	-	-	-	89.7	-	-69.7	-	1.8	64.3	9	7
BA 4	41.3854	23.4218	-	55.7	312.1	-	-	43.0	145.0	-	-57.2	-	119.8	6.1	8	6
BA 5	41.3832	23.4240	-	-	-	-	-	-	161.7	-	-42.4	-	36.4	12.9	8	5
BA 6	41.3820	23.4254	-	57.8	283.1	-	-	29.2	146.6	-	-46.6	-	50.6	8.6	8	7
BA 7	41.3817	23.4354	-	-	-	-	-	-	141.2	-	-40.1	-	22.7	12.9	8	7
BA 8	41.3807	23.4254	054/15	74.5	218.5	-	-	26.3	175.7	-	-44.6	-	393.0	3.0	8	7

Table 2*. AF demagnetization results for sampled volcanics with a promising signal after first thermal demagnetization. 1) - unknown error; λ – latitude pole; φ – longitude pole; palat – paleo-colatitude; ΔD – declination deviation; ΔI – inclination deviation.*

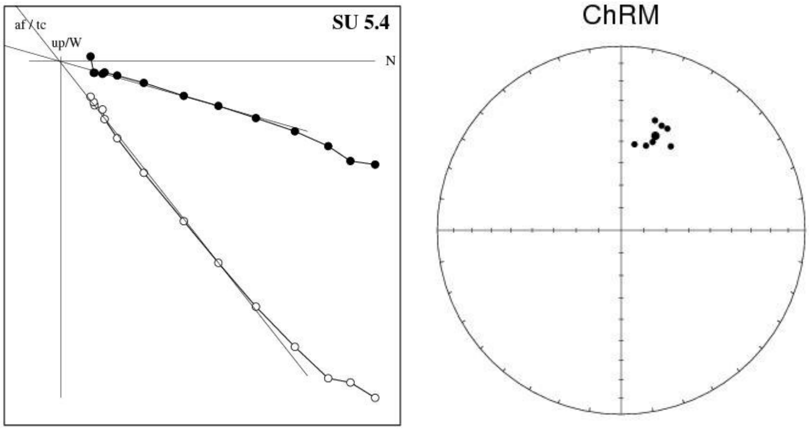

Figure 3a and b. *An example of a normal polarity sample. Demagnetization diagram of sample SU 5.4 and equal area projection of mean directions of ChRM of site SU 5.*

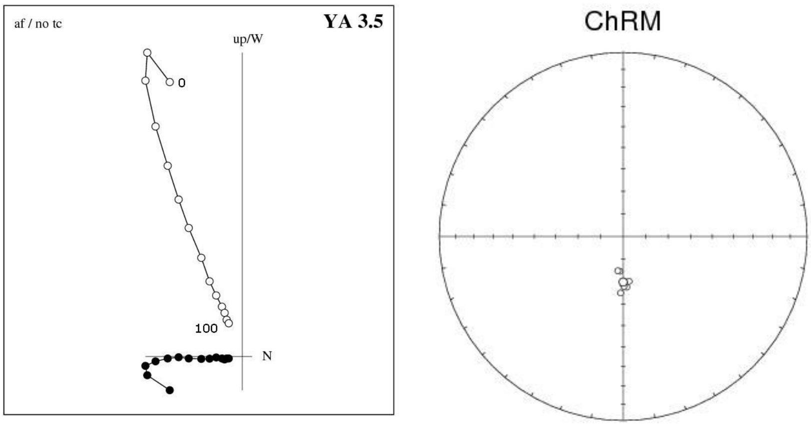

Figure 3c and d. *An example of reversed polarity with an overprint. Demagnetization diagram of sample YA 3.5 and equal area projection of mean directions of ChRM of site YA 3.*

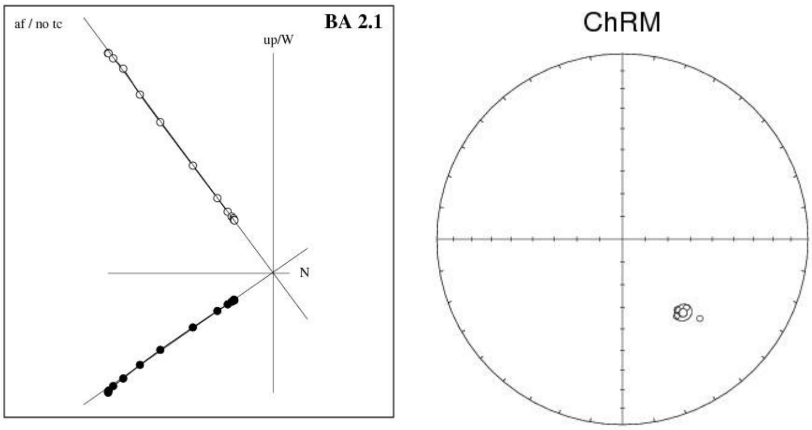

Figure 3e and f. *An example of a reversed polarity sample. Demagnetization diagram of sample BA 2.1 and equal area projection of mean directions of ChRM of site BA 2.*

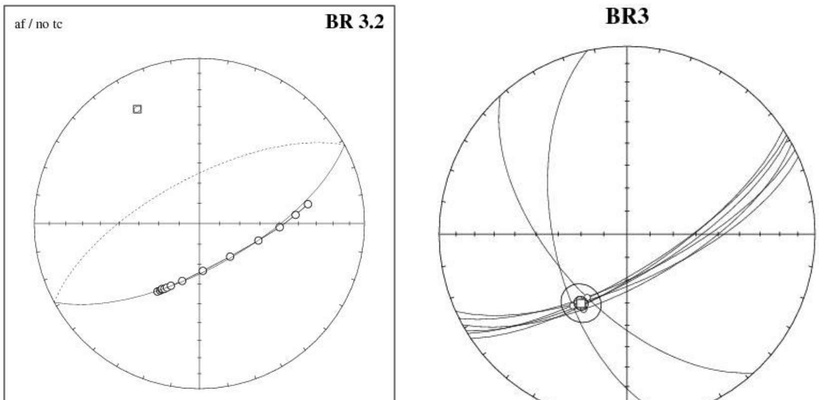

Figure 3g and h. *An example of greatcircles. Demagnetization diagram (equal area projection) of sample BR 3.2 and projection of greatcircles and mean direction of ChRM of site BR 3.*

in demagnetization diagrams of the Yabalkovo lavas. This is shown in figure 3c and d. The Banichan sites give a nice example of reversed polarity demagnetization diagrams, as can be seen in figure 3e and f. Samples from Dospat and Zvesdel have demagnetization diagrams that are quite similar, they only vary slightly in exact direction (SW or SE) and degree of inclination. Samples from Bratsigovo are almost all greatcircles, which were treated in the same way as for the Lukovit sites. Figure 3g and h show an example of a greatcircle and the determination of a site mean direction for Bratsigovo.

As can be seen in table 2, almost all localities show variation, some smaller and some larger, around a paleomagnetic declination of 180^o (thus southward). This is also shown in the overall mean direction of 191.6^o ± 10.4^o. Banichan has a quite different value of 152^o ± 20^o for its mean declination. Bratsigovo also differs much from this mean with a declination of 313^o (and a deviation that could not be calculated due to an unknown error in the spreadsheet). Also, the ΔI of 113.9^o that is calculated for Bratsigovo is impossibly high because one of the three directions is completely different.

In between sites, there is also quite some variation shown in directions and deviations. Dospat is the only site that shows a relatively high ‘success-rate’ with very low deviation rates for both declination and inclination. The other localities have deviations of around 20^o.

An important remark can be made on the results as presented above. As can be seen in the table, a higher number of (good) sites per locality give smaller deviations and thus more reliable results. A higher number of data is necessary to average the influence of secular variation. Only a few directions will not be able to average this variation because outliers will have a relatively large influence on the mean direction.

Calculation of the deviation of the overall outcome relative to the Eurasia reference pole at 30 Ma from Torsvik et al (2008 - in press), gives a mean declination of 175.7^o ± 10.9^o for the Moesian platform and the Bulgarian Rhodope.

3.3. Rock magnetic experiments

Figure 4a to e show the resulting diagrams for the low-field magnetic susceptibility experiments for a sample from five out of six of the volcanic sites. Unfortunately, there are no results for the sample from the Suhindol locality.

The Curie temperature from the dominant ferromagnetic mineral can be determined from the point of major decrease in magnetic susceptibility. As can be seen in the diagrams, all Curie temperatures lie around 580 to 630^{o}C. Titanomagnetites have a T_C of around 580^{o}C, which can be observed in the diagram from BR and, less clearly, from YA. As titanomagnetite is generally the dominant ferromagnetic mineral in igneous rocks, this result is not surprising for volcanic localities like Bratsigovo and Yabalkovo.

The diagrams for Banichan and Dospat both show a somewhat higher T_C of around 610 to 630^{o}C. Those temperatures are typical for ferromagnetic minerals from the titanohematite series. Maghemite has a T_C between 590 and 675^{o}C, and mostly around 600^{o}C (Butler, 1998). Hematite has a higher T_C of around 680^{o}C. With this information, the Curie temperature in the BA and DO diagrams is most likely caused by maghemite. In general, titanohematites are a lesser portion of ferromagnetic minerals present in most igneous rocks. However, they can be the dominant minerals in highly silicic or highly oxidized rocks. Both lavas from Dospat and Banichan have a rhyolitic composition, which is relatively high in silica and can thus explain the occurrence of titanohematites.

The diagram for the sample from the Zvesdel locality (basaltic to andesitic lavas) shows a T_C of around 600^{o}C. This can be caused from either titanomagnetite or titanohematite.

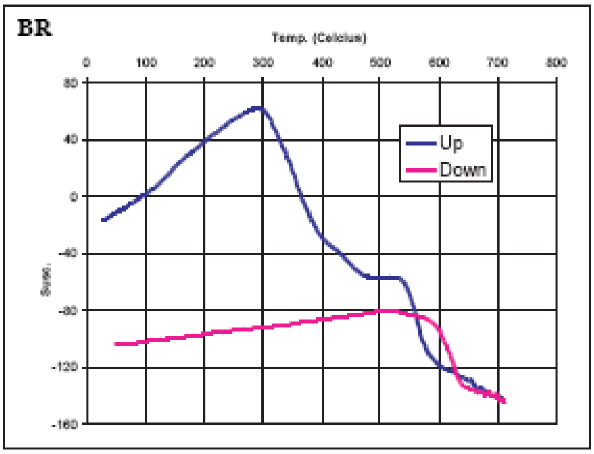

__Figure 4a__. Diagram for low field magnetic susceptibility test for a sample from Bratsigovo. A T_C of around 580^{o}C can be observed.

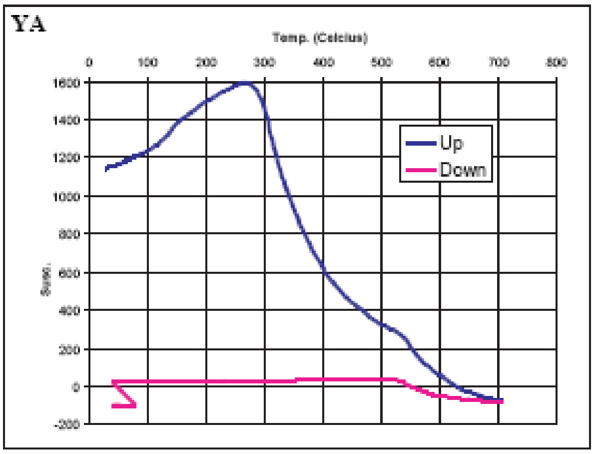

__Figure 4b__. Diagram for low field magnetic susceptibility test for a sample from Yabalkovo. This sample has a T_C of around 580^{o}C.

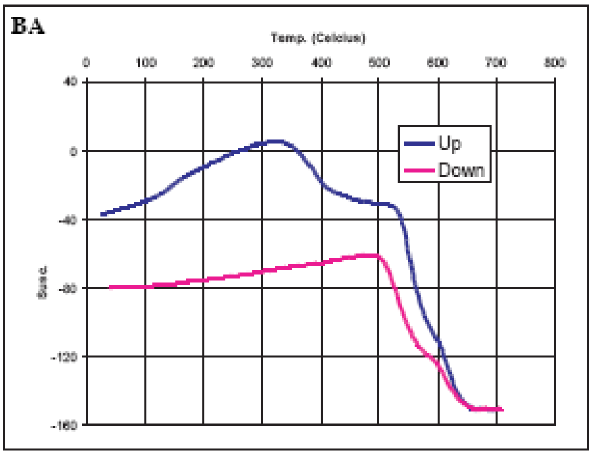

__Figure 4c__. Diagram for low field magnetic susceptibility test for a sample from Banichan. As can be seen, the T_C lies around 610-630^{o}C.

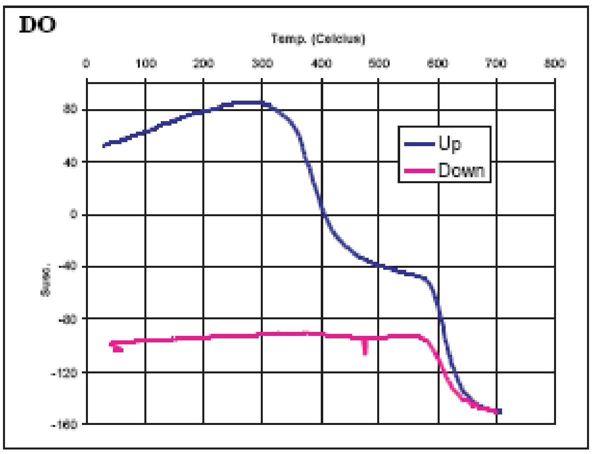

__Figure 4d__. Diagram for low field magnetic susceptibility test for a sample from Dospat. Again, a T_C of around 610 to 630^{o}C can be observed.

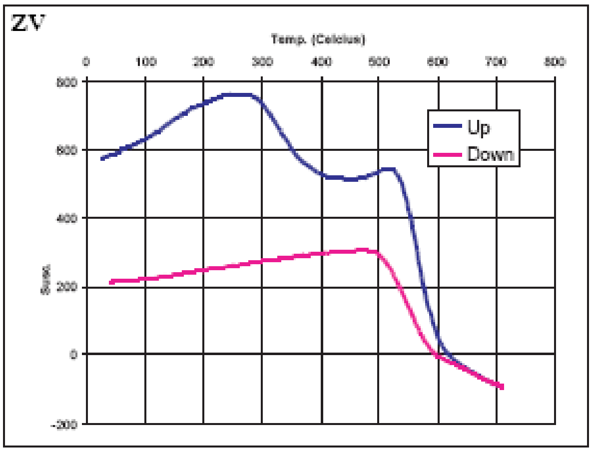

***Figure 4e**. Diagram for low field magnetic susceptibility test for a sample from Zvesdel. The diagram shows a T_C of around 600°C.*

4. Discussion

4.1. Sediments

In general, sediments are less able to preserve a primary NRM well than igneous rocks are, because, for instance, sediments are more easily weathered and magnetized sedimentary particles can also be re-aligned after deposition by disturbances like bioturbation. Sedimentary rocks are more easily influenced by a secondary magnetization phase than the magnetic particles in igneous rocks. Therefore, a paleomagnetic study based on mostly sediment samples is a highly risky business.

As mentioned in the previous chapter, influences from overprinting and magnetic mineral transformation during heating resulted in complicated multiple-component diagrams which were not interpretable. Logically, it is also possible that errors were made during sampling and measuring in the field and in the lab. At several sites, it was necessary to drill in relatively soft rocks, which were not fully consolidated. This made the drilling itself very easy, but the cores were easily turned in their hole and this caused the reliability of the measured orientation and thus of the paleomagnetic direction to decrease.

Other dangers of sampling which can cause unreliable results were already mentioned in paragraph 2.2.

For the Lukovit locality, sites LU2 and 3 give excessively high κ values, which would be high even for uncommon very fresh volcanic rocks. Sites LU5 and 7 give very high $\alpha95$ values. It is possible that these exceptional values are caused by the small number of samples (two to four) that was actually useful for the concerning calculation.

Subsequently, not much can be said about the results of the remaining sedimentary sites, including the sites from Mezdra. This is because the number of rejected samples and sites is too high, causing the reliability of the result of the remaining samples/sites to diminish.

4.2. Volcanics

As mentioned before, igneous rocks have a much higher chance of success in paleomagnetics than sedimentary rocks do. This is because the first are much more resistant against altering processes and secondary remagnetizations that can influence the strength and conceal the direction of the primary NRM. Therefore, deviations in the results from the volcanic sites from this study will be mostly caused by sampling and measuring errors. Apart from the usual measuring errors in the field, this is for instance in the case of a sample that was loosened from its hole before it was measured, or a sample that was drilled in a block that was somewhat loosened from the rest of the outcrop, as was mentioned in paragraph 2.2. Those possible errors contribute to larger deviations from declination and inclination within sites and localities.

Except for errors from overprinting or magnetic mineral transformation during heating, there are some other possible reasons for bad results from the volcanic samples in this study. At some of the localities it was tried to measure a bedding of the host rock surrounding the volcanic plugs. This was not always possible or very difficult. Therefore, it can very well be that bedding-tilt corrections are not fully correct, and that other sites actually needed a bedding-tilt correction while none was observed in the field, which can possibly be the cause of some of the larger deviations in declination and inclination.

All localities except Bratsigovo have quite acceptable confidence levels for their pole. Usually, K values of 10 to 80 are reasonable, together with A95 values of about 15, at most. The latter becomes smaller with an increasing number of considered data. Therefore, it is not strange that both the Zvesdel and the Banichan locality have relatively high A95 values (17°), because of the relatively small number of sites included (five and four).

As mentioned in the last chapter, there is much difference in the determined declination and inclination between the sites of the Bratsigovo locality. This is shown in the extremely low value for the confidence level of the calculated pole, which actually makes the locality 'not acceptable'. Despite of this fact, the locality was used in the calculation for the overall mean pole and direction. The reason that the results from Bratsigovo differ so much from the mean direction calculated can not be explained easily. This is because within the sites, the confidence levels for the results have acceptable values for igneous rocks. It is not likely that within every site, the same measuring error is made. A possible, but very unlikely explanation is that all samples from a certain site are by accident placed in a wrong direction in the AF demagnetizer. Another possibility is the bedding-tilt correction. For the whole Banichan locality, a bedding attitude was measured, which was not done for many other sites from other localities. Possibly this measurement or correction turned out to be not very accurate.

4.3 Geodynamic implications

The calculated mean paleodeclination of all volcanic sites of 191° ± 10.4° at about would imply a minor rotation of the Moesian Platform and the Bulgarian Rhodope since 30 Ma. However, by taking the overall rotation of the continent into consideration by comparing it with the reference pole at 30 Ma shows that the rotation of the Bulgarian region within the continent was negligible (-4.3° ± 10.9°); it fits in the overall rotation and it can therefore be considered as a stable block in between the two rotating systems in the north and south.

Thus, the Miocene rotation of the Aegean and Carpathian regions was hardly or not accommodated by movement of the Bulgarian region.

Schmid et al (1998) concluded that the Late Eocene arc formation in the Southern Carpathians was initiated because of major N-S stretch in this belt due to the movement of the western part of the Rhodope past the Moesian Platform. This stable part acted as a corner during the bending phase, and post-Eocene 50° CW rotation of the Southern Carpathians (around a pole in the Moesian Platform) and dextral wrenching along the boundary was indeed not accommodated in the Platform.

5. Conclusion

Sampled sediments from the Moesian Platform almost all gave useless results, whereas very good results came out of the large part of the volcanics, mostly sampled in the Bulgarian Rhodope.

According to the paleomagnetic results in this study, the Moesian Platform and the Bulgarian Rhodope underwent a paleomagnetic direction of 11° ± 10.4° North at 30 Ma. With respect to the Eurasian paleopole, this rotation becomes negligible with respect to the overall movement of the Eurasian continent, comparing it with the reference pole of the continent at 30 Ma: only 4.3° ± 10.9° CCW. Thus, the Bulgarian region proves to be a stable block during the major rotations of the Carpathian arc in the north and the Aegean region in the south since 13 Ma.

Low-field magnetic susceptibility experiments show that the dominant ferromagnetic minerals in the volcanic samples are titanomagnetite, and most likely maghemite for a few localities that consisted of highly silicic lavas.

References

Butler, R.F., 1998. "Paleomnagnetism: Magnetic Domains to Geologic Terranes." Electronic Edition.

Dupont-Nivet, G., Vasiliev, I., Langereis, C.G., Krijgsman, W., Panaiotu, C., 2005. "Neogene tectonic evolution of the southern and eastern Carpathians constrained by paleomagnetism." Earth and Planetary Science Letters **236**: p. 374-387.

Georgiev, G., Seghedi, A., co-workers, 2000. "IGCP Project no. 369: Comparative Evolution of PeriTehyan Rift Basins." *http://www-sst.unil.ch/igcp_369/369_ text/igcp369_moesia.htm*

Jordanova, N., Henry, B., Jordanova, D., Ivanov, Z., Dimov, D., Bergerat, F., 2001. "Paleomagnetism in northwestern Bulgaria: geological implications of widespread remagnetization." Tectonophysics **343**: p. 79-92.

Schmid, S.M., Berza, T., Diaconescu, V., Froitzheim, N., Fugenschuh, B., 1998. "Orogen-parallel extension in the Southern Carpathians." Tectonophysics, **297** (1-4), p. 209-228.

Torsvik, T.H., Dietmar Müller, R., Van der Voo, R., Steinberger, B., and Gaina, C., 2008. "Global plate motion frames: toward a unified model." Reviews of Geophysics, in press.

Van Hinsbergen, D.J.J., Langereis, C.G., Meulenkamp, J.E., 2005. "Revision of the timing, magnitude and distribution of Neogene rotations in the western Aegean region." Tectonophysics **396**: p. 1-34.

Earth and Planetary Science Letters xxx (2008) xxx–xxx

Contents lists available at ScienceDirect

Earth and Planetary Science Letters

journal homepage: www.elsevier.com/locate/epsl

No significant post-Eocene rotation of the Moesian Platform and Rhodope (Bulgaria): Implications for the kinematic evolution of the Carpathian and Aegean arcs

Douwe J.J. van Hinsbergen [a,*], Guillaume Dupont-Nivet [a], Radoslav Nakov [b], Karen Oud [a], Christian Panaiotu [c]

[a] Paleomagnetic Laboratory 'Fort Hoofddijk', Utrecht University, Budapestlaan 17, 3584 CD Utrecht, The Netherlands
[b] Geological Institute, Bulgarian Academy of Sciences, Acad. G. Bonchev St., Bl. 24, 1113 Sofia, Bulgaria
[c] University of Bucharest, Paleomagnetic Laboratory, Balcescu 1, Bucharest, Romania

ARTICLE INFO

Article history:
Received 25 February 2008
Received in revised form 26 June 2008
Accepted 29 June 2008
Available online xxxx

Editor: C.P. Jaupart

Keywords:
Paleomagnetism
rotation
tectonics
kinematics
Mediterranean
Rhodope

ABSTRACT

The region located between the Carpathian–Balkan and Aegean arcs, the Moesian Platform and Bulgarian Rhodope, is generally assumed to have been stably attached to the East European craton during the Cenozoic evolution of these arcs. The kinematic evolution of this region is, however, poorly constrained by paleomagnetic analysis. In this paper we provide new paleomagnetic data (800 volcanic and sedimentary samples from 12 localities) showing no significant post-Eocene rotation of the Moesian platform and Rhodope with respect to Eurasia, therefore confirming the stability of this region. We compare this result to a provided review of paleomagnetic data from the South Carpathians (Tisza block) and the Aegean region. The Tisza block underwent 68.4 ± 16.7° of middle Miocene (~15–10 Ma) clockwise rotation with respect to the Moesian Platform, in line with previous rotation estimates based on structural geology. The stability of the Moesian platform during middle Miocene eastward emplacement of the Tisza block into the Carpathian back-arc supports dextral shear along the Southern Carpathians recorded by 13–6 Ma clockwise strike-slip related rotations in foreland deposits. The new reference direction for the Moesian platform and Rhodope allows accurate quantification of the rotation difference with the west Aegean domain at 38.0 ± 7.2° occurring between 15 and 8 Ma. To accommodate this rotation, we propose that the pivot point of the west-Aegean rotation was located approximately in the middle of the rotating domain rather than at the northern tip as previously proposed. This new scenario predicts less extension southeast of the pivot point, in good agreement with estimates from Aegean structural geology. Northwest of the pivot point, the model requires contraction or extrusion that can be accommodated by the coeval motion of the Tisza Block around the northwestern edge of the Moesian platform.

1. Introduction

The mountain belts that evolved in southeastern Europe have served as type localities for the development of general concepts for mountain building, orogenic collapse and subducted slab dynamics: the Aegean, Carpathian and Balkan orogenic systems (Fig. 1). Between the Carpathian and Balkan orogenic systems is the Moesian Platform, a Precambrian basement block that is generally regarded to belong to stable Europe. It is therefore used as an essential reference for kinematic reconstructions during the Cenozoic (e.g. Linzer, 1996; Morley, 1996; Linzer et al., 1998; Ricou et al., 1998; Schmid et al., 1998; Zweigel et al., 1998; Fig. 1). However, the tectonic stability of this block during the evolution of the Carpathian, Balkan and Aegean systems is questionable and still poorly constrained by reliable paleomagnetic studies of vertical-axis rotation.

In regions adjacent to the Moesian Platform, large vertical-axis block rotations have been determined paleomagnetically, allowing to constrain and quantify Cenozoic kinematics (Horner and Freeman, 1983; Balla, 1987; Kissel and Laj, 1988; Morris, 1995; Speranza et al., 1995; Kissel et al., 2003; Csontos and Voros, 2004; van Hinsbergen et al., 2005a). To the north in the Carpathian region, ~80° of clockwise rotations in the large Tisza Block since the Oligocene are generally interpreted to reflect its wholesale motion around the northwestern corner of the Moesian Platform during eastward roll-back of the Carpathian subducted slab (e.g. Patrascu et al., 1994; Panaiotu, 1998; Schmid et al., 1998). To the south, the entire domain formed by the western Aegean and Albanian regions, rotated 50° clockwise (away from the Northern Rhodopes and the Moesian Platform) largely between ~15 and 8 Ma. This has been interpreted to be caused by a combination of southward roll-back of the African slab and/or westward extrusion of Anatolia (Kissel and Laj, 1988; Kissel et al., 2003; van Hinsbergen et al., 2005a). These interpretations, however, rely on the assumption that the Moesian Platform has not rotated during the rotation of these domains. To date, paleomagnetic information from the Moesian Platform is scarce, but does suggest some Cenozoic rotation (Dolapchieva, 1994). Recently acquired results from the Moesian Platform itself suggest a ~15° clockwise rotation of

* Corresponding author. Tel.: +31 30 2531676.
E-mail address: hins@geo.uu.nl (D.J.J. van Hinsbergen).

0012-821X/$ – see front matter © 2008 Elsevier B.V. All rights reserved.
doi:10.1016/j.epsl.2008.06.051

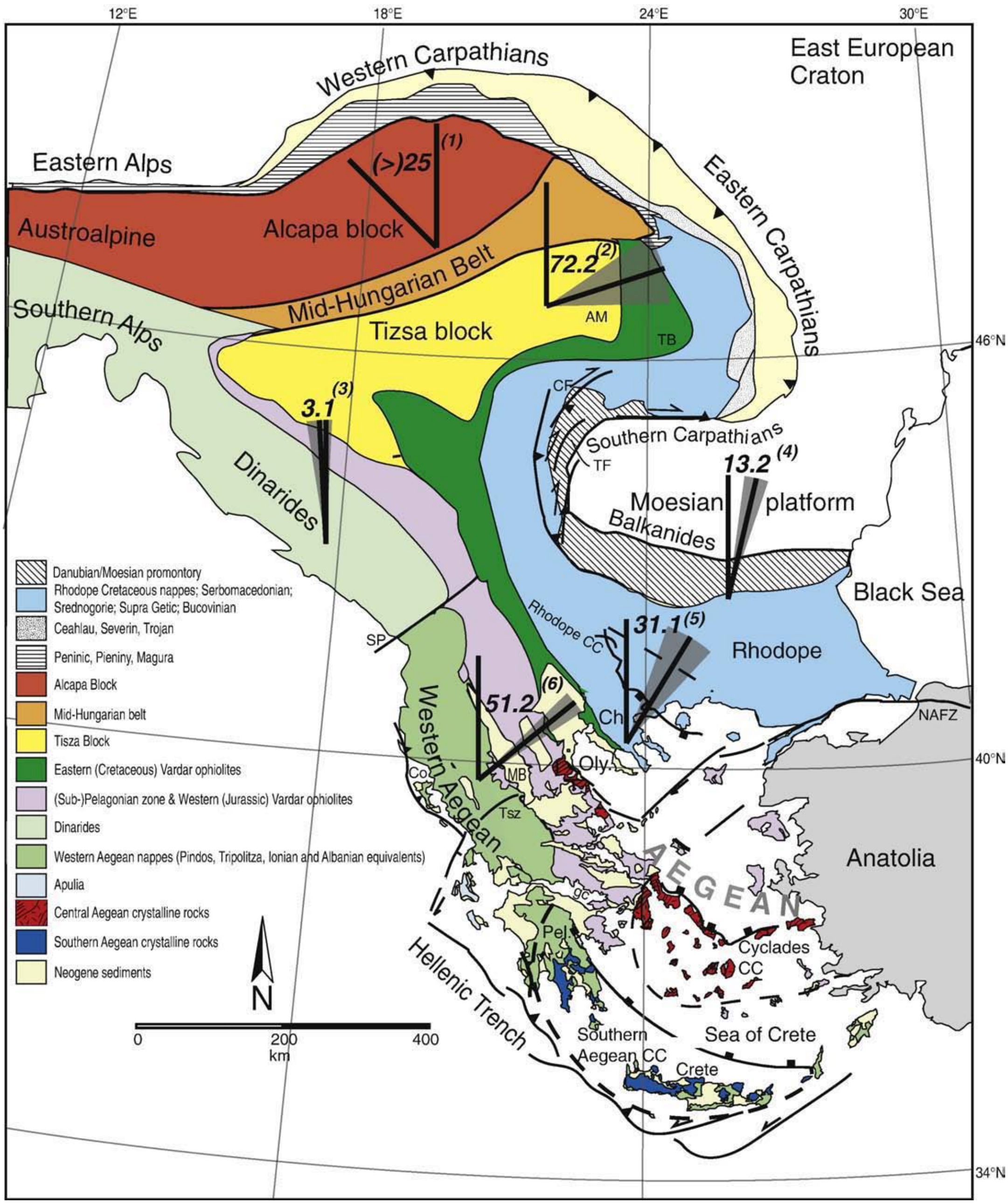

Fig. 1. Schematic geological map with the main tectonostratigraphic units of the southeastern Europe, with the declinations obtained from the Eo-Oligocene of the main blocks of the region. References for the composite declinations constructed from the available literature: 1. Alcapa-block—we adopt the ~25° counterclockwise rotation argued for on structural/palinspastic basis by Ustaszewski et al. (in press). See this reference for discussion and review of the paleomagnetic and structural data; 2. Tisza Block—see Appendix A; 3. Dinarides—data from Kissel et al. (1995), see Appendix A; 4. Moesian Platform and Bulgarian Rhodope—This study; 5. Chalkidiki Peninsula—data from Kondopoulou and Westphal (1986), see Appendix A; 6. Western Greece and Albania—see Appendix A for data and references. Map modified after van Hinsbergen et al. (2005c) and Schmid et al. (2008). AM = Apuseni Mountains; CC = crystalline complex; CF = Cerna-Jiu Fault; Ch = Chalkidiki peninsula; gc = Gulf of Corinth; MB = Mesohellenic Basin; SP = Scutari-Pec Transform Fault; TB = Transylvanian Basin; TF = Timok Fault; Tsz = Thesprotiko Shear Zone.

the Platform during or after early to mid-Eocene contractional tectonics and remagnetisation (Jordanova et al., 2001). Along the northern margin of the Moesian Platform, the foreland basin sediments of the southern Carpathians, record a phase of 30° clockwise rotation between 13 and 6 Ma (Dupont-Nivet et al., 2005). This rotation phase is justifiably interpreted to relate to dextral shear associated with the eastward emplacement of the Tisza block, assuming the Moesian Platform did not rotate. However, another speculative interpretation—not excluded by existing constraints—is that the Tisza block and the Southern Carpathians rotated clockwise together with the Moesian Platform between 13 and 6 Ma. The fact that this rotation phase is contemporaneous with the west Aegean rotations, further suggests that the Tisza block and the western Aegean region may have (partly) rotated together. This would have major implications for the loci of kinematic (extensional) accommodation of the Aegean and Carpathian block rotations (i.e. the west-Aegean rotations may have been partly accommodated in the Carpathian back-arc). Assessing the rotation of the Moesian Platform is therefore a key element that is still missing to test these different hypotheses for the southeastern European geodynamics. In this study, we provide new paleomagnetic from the Moesian Platform and Bulgarian Rhodope to quantify its rotation since Eocene time and discuss the implications of our new findings for the kinematic evolution of the Carpathian and Aegean arcs.

Please cite this article as: van Hinsbergen, D.J.J., et al., No significant post-Eocene rotation of the Moesian Platform and Rhodope (Bulgaria): Implications for the kinematic evolution of the Carpathian and Aegean arcs, Earth Planet. Sci. Lett. (2008), doi:10.1016/j.epsl.2008.06.051

2. Geological setting

The Moesian Platform extends over large parts of Bulgaria and Romania, from the southern Carpathians in the north, to the Balkan fold-and-thrust belt (Balkanides) in the south (Fig. 1). Its metamorphic basement is covered by >10 km of lower Paleozoic to Recent sediments and some volcanics (Carboniferous–Permian, Triassic and Miocene) (Tari et al., 1997). Alpine deformation over the southern margin of the Moesian Platform was associated with the northward emplacement of the Balkanides and Srednogorie nappes in a back-thrust system associated with northward subduction during Africa–Europe convergence (Boccaletti et al., 1974; Ricou et al., 1998; van Hinsbergen et al., 2005b), leading to an upper Cretaceous to Paleogene foreland basin stratigraphy covering the Platform (Tari et al., 1997). The contractional deformation along the southern edge of the Platform ended during the middle Eocene along most of its length, although some local contraction in the southeastern part continued in the Oligocene (Sinclair et al., 1997). The Rhodope forms a complex structure including exhumed high-grade metamorphic rocks buried and exhumed during the Cretaceous to Paleogene (and in northern Greece into the Oligo-Miocene) (Ricou et al., 1998; Brun and Sokoutis, 2007), overlain by Eocene to Oligocene sedimentary basins and volcanic fields (Lilov et al., 1987; Yanev and Pecskay, 1997; Yanev et al., 1998; Fig. 2). Significant contraction south of the Moesian Platform ended in the Eocene (e.g. Ricou et al., 1998), after which the loci of deformation shifted to the south as accretion migrated southward (van Hinsbergen et al., 2005c). By this time, the Rhodope had accreted to the Moesian Platform as indicated by the absence of major post-Eocene structures that could have accommodated significant motion (rotation or translation) between these blocks. Post-middle Eocene exhumation in the Rhodope was largely accommodated by tectonic denudation in core complexes occurring south of the volcanic fields of the Bulgarian Rhodope (Dinter and Royden, 1993; Ricou et al., 1998; Krohe and Mposkos, 2002; Brun and Sokoutis, 2007). This extensional history has formed a series of post-middle Eocene grabens and half-grabens in the southern Rhodope (e.g. the middle-late Miocene Struma (or Strimon) and middle Eocene Mesta grabens) cross-cutting the pre-Eocene nappe stack (Tzankov et al., 1996; Nakov, 2001; Burchfiel et al., 2003).

Along the northern margin of the Platform—south of the Carpathians—late Cretaceous nappe stacking is followed by significant post-Eocene deformation (Fügenschuh and Schmid, 2005). Although contractional deformation along the southern margin of the Moesian Platform ended in the Eocene, the western and northern margins were subjected to overthrusting and right-lateral wrenching associated with northward and eastward propagation of the Carpathian fold-and-thrust belt around the Moesian Platform from Eocene to Pliocene time (ending in the late Miocene in the Southern Carpathians, and Pliocene in the Eastern Carpathians) (Schmid et al., 1998; Bertotti et al., 2003; Matenco et al., 2003; Dupont-Nivet et al., 2005; Vasiliev et al., 2005). This north-eastwards migration of the Carpathian arc is believed to result from eastward slab roll-back of (oceanic?) lithosphere that occupied the present Carpathian–Pannonian region (Carpathian embayment) prior to subduction (Linzer et al., 1998; Schmid et al., 1998; Wortel and Spakman, 2000; Csontos and Voros, 2004). Arc migration was stopped by subsequent continental collision between the accreted allochthonous terranes and the East European cratonic margin (Morley, 1996; Linzer et al., 1998; Zweigel et al., 1998; Matenco and Bertotti, 2000; Fig. 1). In this context, the southern Carpathians have been interpreted as a subduction transform edge propagator (STEP) fault (Govers and Wortel, 2005). The formation of the Carpathians resulted in a distinctive depositional pattern of thick Miocene to Pliocene foreland deposits on the Moesian Platform that are exposed in thrust sheets along the Southern Carpathians. Basin analysis and modeling indicates accelerated subsidence during the early to middle Miocene time followed by a climax of subsidence between ~13 and 9 Ma (Bertotti et al., 2003; Matenco et al., 2003; Cloetingh et al., 2004). In summary, the Moesian platform was, in the south, overthrusted and deformed until mid-Eocene times due to subduction/collision processes in the Aegean arc, and, along its northern margin, transpressionally deformed by eastward propagation of the Carpathian arc mainly during Miocene times.

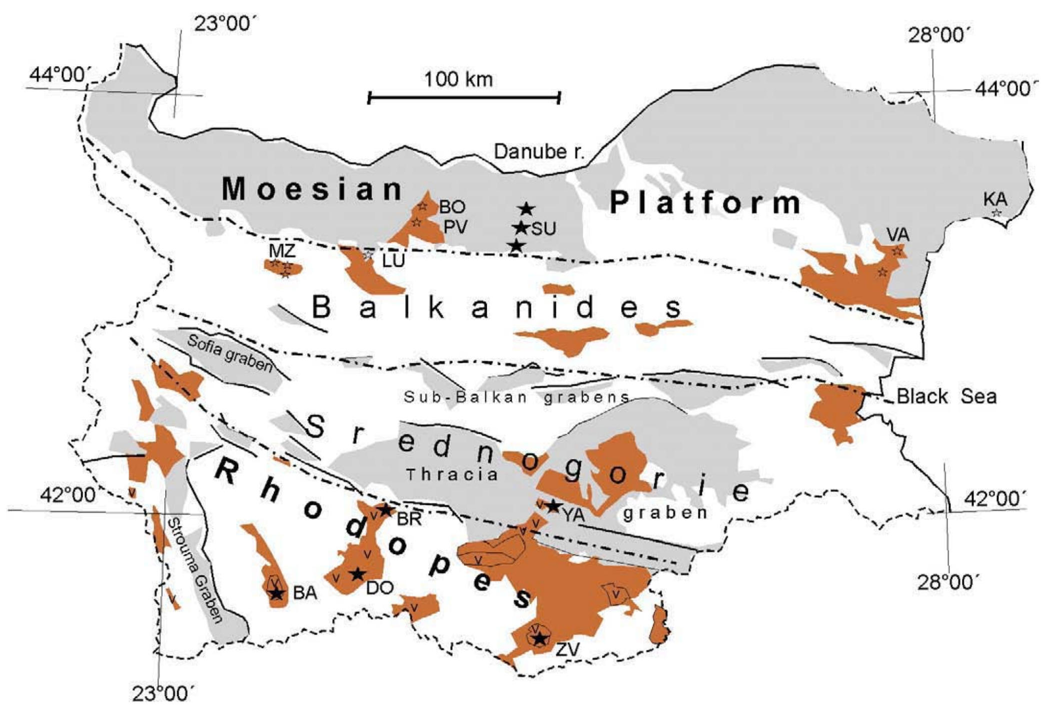

Fig. 2. Structural sketch-map of Bulgaria with shown post-Cretaceous rock. Light (grey)—Neogene–Quaternary sediments (except some locally occurring basalts in central North Bulgaria—sites Suhindol (SU)); Dark (orange)—Paleogene rocks, locally including lower Miocene (Thracia graben and western Bulgaria); v—volcanics; Thick lines—middle Miocene to present extensional faults, forming grabens; dashed line—boundaries of tectonic units; MZ, LU, PV, BO, SU, KA, VA, YA, BR, DO, ZV, BA—sampled localities, fore precise coordinates and names see Table 1 and Appendix A; Filled star—successful site; unfilled—unsuccessful site.

Please cite this article as: van Hinsbergen, D.J.J., et al., No significant post-Eocene rotation of the Moesian Platform and Rhodope (Bulgaria): Implications for the kinematic evolution of the Carpathian and Aegean arcs, Earth Planet. Sci. Lett. (2008), doi:10.1016/j.epsl.2008.06.051

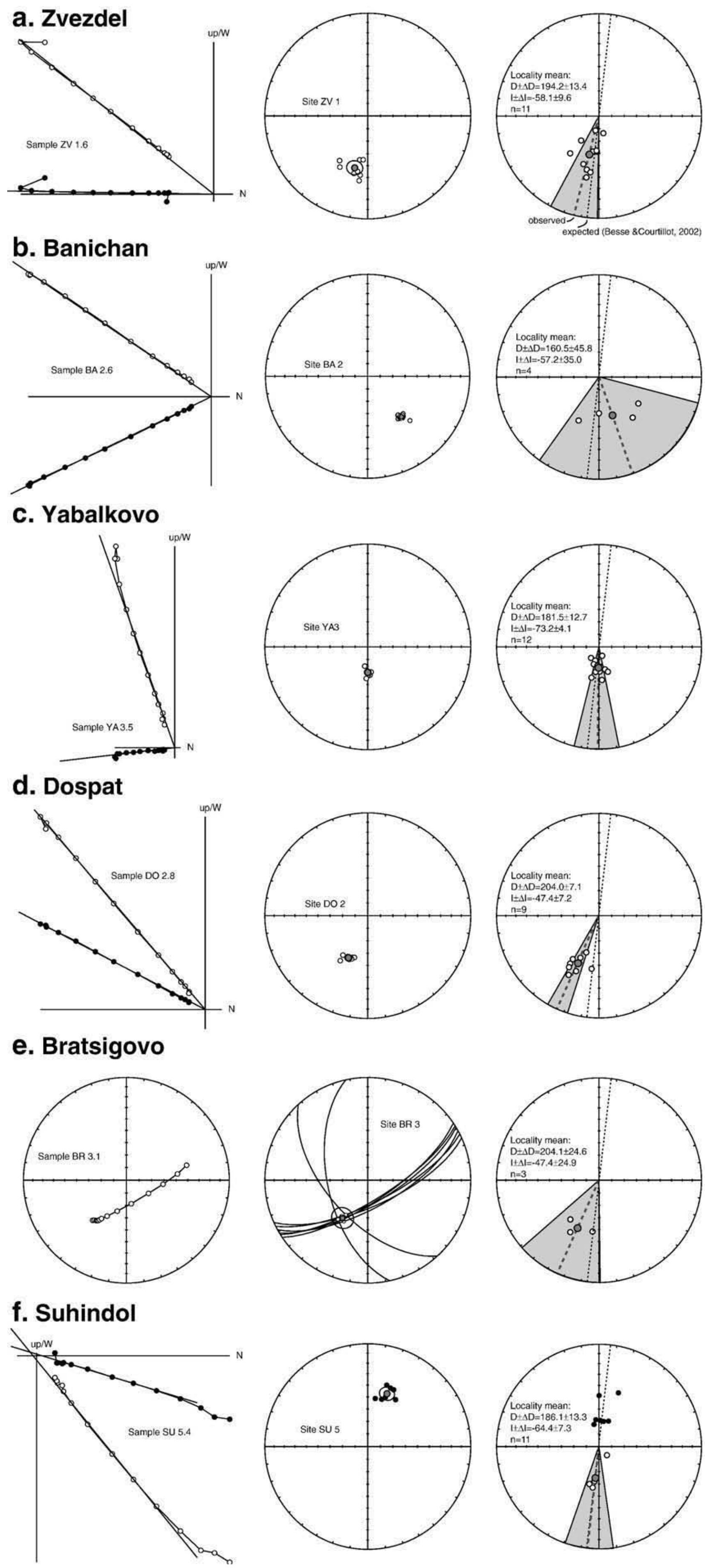
a. Zvezdel
up/W
Sample ZV 1.6
N
Site ZV 1
Locality mean:
D±ΔD=194.2±13.4
I±ΔI=-58.1±9.6
n=11
observed
expected (Besse &Courtillot, 2002)
b. Banichan
up/W
Sample BA 2.6
N
Site BA 2
Locality mean:
D±ΔD=160.5±45.8
I±ΔI=-57.2±35.0
n=4
c. Yabalkovo
up/W
Sample YA3.5
N
Site YA3
Locality mean:
D±ΔD=181.5±12.7
I±ΔI=-73.2±4.1
n=12
d. Dospat
up/W
Sample DO 2.8
N
Site DO 2
Locality mean:
D±ΔD=204.0±7.1
I±ΔI=-47.4±7.2
n=9
e. Bratsigovo
Sample BR 3.1
Site BR 3
Locality mean:
D±ΔD=204.1±24.6
I±ΔI=-47.4±24.9
n=3
f. Suhindol
up/W
N
Sample SU 5.4
Site SU 5
Locality mean:
D±ΔD=186.1±13.3
I±ΔI=-64.4±7.3
n=11

3. Paleomagnetic sampling

To test whether the Moesian Platform can indeed be considered as stable in the Cenozoic, we sampled upper Cretaceous and younger sediments in the central region of the Moesian Platform (away from deformation at the periphery) where they are found mostly undeformed with subhorizontal bedding orientations (Tari et al., 1997). Because most of these sediments are platform carbonates and marls, which may poorly record the paleomagnetic field, we also sampled lower Miocene volcanic rocks exposed on the central Moesian Platform as well as Eocene to Oligocene volcanoes on the Bulgarian Rhodope, to ensure successful results. As outlined above, the thrusts emplacing the Rhodope and underlying nappes over the Moesian Platform predate the flat-lying volcanic field of the Rhodope. In addition, post-Eocene extensional exhumation phases and associated vertical-axis rotations occur only south of the Bulgarian volcanic fields, e.g. between the Chalkidiki peninsula and the Rhodope, on either side of the Strimon detachment (Kondopoulou and Westphal, 1986; Dimitriadis et al., 1998; Brun and Sokoutis, 2007). Therefore, there are no reasons to expect regional rotation differences between the Rhodope and the Moesian Platform after the Eocene.

We collected approximately 800 samples from 12 localities on the Moesian Platform and Bulgarian Rhodope (Fig. 2). Paleomagnetic samples were collected with a hand-held gasoline-powered drill with water-cooled diamond-coated drill bits. The orientation of all samples was measured with a magnetic compass, and corrected for local declination (4°). Six localities were sampled in upper Cretaceous–Paleocene (Mezdra, Bojouritsa), Eocene (Varna, Pleven) and Miocene (Lukovit, Kavarna) sedimentary rocks of the Moesian Platform. Additionally, we collected (in most cases eight) samples from a total of 58 lava sites in six localities. Twelve sites were sampled in three lower Miocene volcanic plugs (24.0–19.4 Ma K/Ar ages: Yanev et al., 1993) at a locality north of Suhindol (Butovo, Dragomirovo, Chervena; Fig. 2). Although the host sedimentary rocks in which these plugs intruded are not well exposed here, their position in the heart of the Moesian Platform (where observed post-Eocene tilts nowhere exceed 5°), leads us to assume that they did not undergo significant post-emplacement tilting. Furthermore, we collected flat-lying volcanics (lavas and ignimbrites) from volcanoes in the Bulgarian Rhodope. A wealth of K/Ar and Ar/Ar ages have been published for these volcanic rocks, generally clustering between ~31 and 37 Ma, with younger dike swarms down to 25 Ma (Lilov et al., 1987; Yanev and Pecskay, 1997; Yanev et al., 1998; Pecskay et al., 2000). Volcanism in the nearby Greek Rhodope has yielded comparable ages, ranging from ~25 to 31 Ma (Innocenti et al., 1984). Three of the volcanic centers that we have sampled have published ages: Zvezdel (twelve lava sites), with ages of 31–33 Ma (Lilov et al., 1987), and our locality Yabalkovo (twelve lava sites), with ages of 31.5–35 Ma (Lilov et al., 1987). Three other localities were sampled in felsic volcanics of Bratsigovo (four ignimbrite sites), Dospat (ten ignimbrite sites) and the lavas of Banichan (eight lava sites with an age of 28–29 Ma: Pecskay et al., 2000) in the western part of the Rhodope Mountains.

4. Paleomagnetic analysis

4.1. Rock magnetism and sample treatment

For all samples, the natural remanent magnetisation (NRM) of the specimens was measured on a 2G Enterprises horizontal DC SQUID cryogenic magnetometer (noise level 3×10^{-12} Am^2). The samples were demagnetized stepwise using either thermal (TH) demagnetization for sediments or alternating field (AF) demagnetization for volcanic rocks. Heating took place in a magnetically shielded, laboratory-built furnace using small temperature increments of 30–80 °C. Unfortunately, none of the demagnetizations from the sedimentary sites yielded interpretable paleomagnetic directions, which is mainly the result of very low initial intensities. In Appendix A, we give the GPS coordinates of the sedimentary sites. For the volcanic rocks, AF demagnetization was carried out with 5–20 mT increments up to 120 mT with a degausser interfaced with the magnetometer by a laboratory-built automated measuring device. Identification of the characteristic remanent magnetization (ChRM) was done upon inspection of decay curves, equal-area projections and vector end-point diagrams (Zijderveld, 1967; Fig. 3). Initial intensities range typically from 0.5 to 2.0 A/m. For the volcanic rocks, results reveal fairly simple demagnetization behavior. Within a few sites, one or several samples indicate an overlapping overprint of abnormally high magnetic intensity with random directions likely related to lightning strikes (Fig. 3e). In most samples, however, univectorial decay towards the origin of 90% of the NRM occurs between 15 and 70 mT and is thus defined as the ChRM. This range of unblocking applied AF is typical for titanomagnetite or titanomaghaemite coercivities (Dunlop and Özdemir, 1997). To assess the magnetic mineralogy of the ChRM, the variation of low-field magnetic susceptibility of volcanic rocks from 40 °C to 700 °C has been studied on some representative samples using a KLY3 Kappabridge susceptibility meter with attached CS-3 furnace (Fig. 4). Crushed powder material (~200 mg) was taken from one characteristic specimen from each locality, and was heated and cooled in air in two successive cycles: 40–400–40 °C and 40–700–40 °C. During heating, a moderate increase of susceptibility between 40 and ~300 °C, is followed by a decreases between ~300 and ~400 °C and a sharp decrease between ~525 and 580 °C. During cooling, the variations observed during heating in the lower temperature range (40–400 °C) are not reversible. In contrast, variations in the higher temperature range are reversible. The reversible decrease above 525 °C clearly corresponds to Ti-poor titanomagnetite—probably magnetite—with a Curie temperature close to 580 °C. The lower temperature irreversible variations can be related to titanomaghaemite (rather than Ti-rich titanomagnetite which would result in reversibility at these temperatures (e.g. Biggin et al., 2007)). Titanomaghaemite can result from secondary alteration such as often found in basaltic rocks (e.g. Zhao et al., 2006). The fact that the total intensity is lower after cycling suggests low-Ti titanomaghaemite or maghaemite which inverts to haematite upon heating (rather than Ti-rich titanomaghaemite that would invert to magnetite (Dunlop and Özdemir, 1997)). The lack of secondary directions in the demagnetization diagrams, strongly suggest that maghaemitization did not alter the original paleomagnetic signal carried by Ti-poor titanomagnetite.

4.2. ChRM direction analysis

The few lava sites affected by lightning have within-site randomness of NRM directions and demagnetization paths along great circles that could be identified on equal-area projections and interpreted using the great-circle analysis of McFadden and McElhinny (1988). Otherwise, the most of ChRM directions were calculated by principal component analysis (Kirschvink, 1980). ChRM directions with maximum angular deviation exceeding 15° were rejected from further

Fig. 3. Paleomagnetic results for each locality. Left column shows typical AF demagnetisations (steps in mT: 0, 5, 10, 15, 20, 25, 30, 40, 50, 60, 70, 80, 90, 100) on vector end-point diagrams with solid (open) symbols for projection on the horizontal (vertical) plane. Lines indicates least square line fit (Kirschvink, 1980), except for e. showing equal-area stereographic projection of demagnetisation path along great circle. Central column shows typical site equal-area projection of ChRM directions in upper (open symbols) and lower (solid symbols) hemisphere. Right column shows site-mean directions (all transformed to normal polarity orientation) with associated locality averages (D=declination, I=inclination, ΔD=95% confidence in declination, ΔI=95% confidence in inclination, n=number sites). All results are given in tilt-corrected coordinates. Data and statistical parameters are given in Table 1.

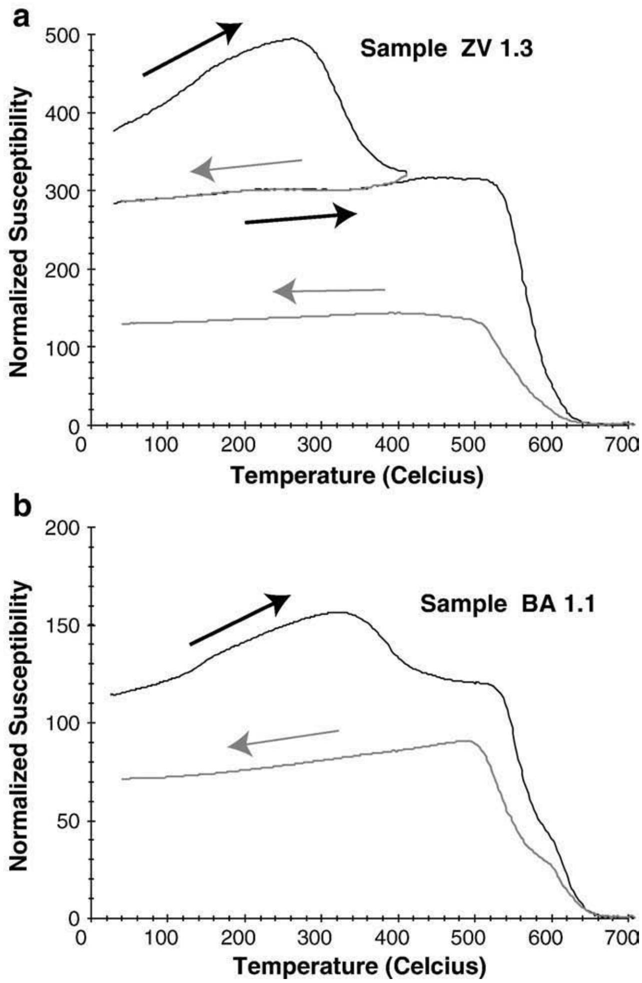

Fig. 4. Typical weak field thermomagnetic curves of normalised susceptibility for representative samples during cycles of heating and subsequent cooling (indicated by arrows). (a) two cycles at 40–400–40 °C and then 40–700–40 °C; (b) one cycle at 40–700–40 °C, see text.

analysis. For each site, the Vandamme (1994) cut-off was applied to discard widely outlying ChRM directions. Averages and cones of confidence on lava site-mean directions were determined using Fisher (1953) statistics assuming random within-site errors (Table 1). We applied a stringent cut-off, rejecting lava site-means with $k<50$, since expected within-site scatter in a lava recording a spot-reading of the Earth's magnetic field should be minimal. In total, 393 samples from 51 sites from six volcanic localities provided conclusive directions, or well-constrained great circles (Table 1). Two sites from the ignimbritic Dospat locality sharing a common true mean direction at the A level of McFadden and Lowes (1981) were combined into one site on the basis that they probably represent the same spot-reading of the magnetic field. This may result from the same ignimbrite being inadvertently sampled twice or two ignimbrites formed within years or tens of years. Application of the fold test is precluded by the absence of sufficient bedding-tilt within and between localities. The outcome of the parametric reversals test of Tauxe (1998) is positive with 95% confidence for the Suhindal locality recording dual polarity (all other localities have exclusively reverse polarity), supporting a primary origin for the magnetisation. For each site-mean direction, the associated Virtual Geomagnetic Pole (VGP) position was calculated. For each locality and for all sites combined, the average VGP with associated 95% confidence circle (A95) was calculated using Fisher statistics (Fisher, 1953); Table 1). Within each locality, the relatively low amounts of VGPs (3 to 12) do not provide sufficient sampling of the geomagnetic field to confidently average out secular variation. In contrast, a meaningful number of sites to average out secular variation is provided by combining our 50 site-VGPs to construct a single VGP for the Moesian Platform and the Bulgarian Rhodope. After exclusion of two outlying VGPs using the Vandamme (1994) cut-off, the remaining 48 site-VGPs yield a late Eocene–early Oligocene pole for the Moesian Platform and Bulgarian Rhodope ($\lambda=80.2°$N; $\varphi=96.9°$E; $A_{95}=4.8°$; $K=19.3$; Scatter = 18.8). This VGP is statistically indistinguishable from the Eurasian Apparent Polar Wander Path (APWP) of this time of Besse and Courtillot (2002) ($\lambda=82.8°$N; $\varphi=158.1°$E; $A_{95}=3.8°$), Schettino and Scotese (2005) ($\lambda=84.1°$N; $\varphi=175.8°$E; $A_{95}=8.1°$) and Torsvik et al. (in press) ($\lambda=82.7°$N; $\varphi=152.5°$E; $A_{95}=2.8°$). In addition, the obtained VGP scatter is comparable to geomagnetic field model predictions for scatter values at this latitude (McFadden et al., 1991). Together with the positive reversals test and the rock magnetic analysis, these observations strongly suggest our results record primary magnetisations providing suitable directions for rotational analysis.

4.3. Rotation analysis

To estimate the possible rotation with respect to a stable reference, we compare VGPs to existing Eocene to Oligocene APWPs of Eurasia at 20 and 30 Ma (Figure Plots). Observed inclination and declination with associated ΔD and ΔI (the error bars on the declination and inclination, respectively, calculated through Eqs. A.60 and A.57 in Bulter (1992)) are compared to expected declination and inclination calculated from the APWPs at an average sampling location (41.56°N, 25.33°E). Based on our dataset, we have no ground to suspect significant rotation differences between our localities. Locality-mean declinations are within 95% confidence intervals of each other and statistically indistinguishable from declinations expected by APWP of stable Eurasia except for a slight offset of the Dospat ($D\pm\Delta D=203.9\pm6.2°$) locality with respect to Yabalkovo locality ($D\pm\Delta D=181.5\pm12.7°$; see Fig. 3). However, comparison between locality-mean directions can be considered meaningless in terms or rotation or absence of rotation, because any directional difference can easily be the result of secular variation not averaged out by the insufficient number of sites within each locality. Consequently, the slight declination offset from the locality Dospat may result from insufficient sampling of secular variation (as suggested by the lower scatter for this locality), and should not be taken as hard evidence for a local rotation with respect to other localities. Moreover, significant rotations between our localities would result in higher than expected scatter values for the overall VGP of the Moesian Platform and Bulgarian Rhodope that averages all our site-VGPs. As noticed above, the scatter associated with this VGP is not higher than the expected scatter values, and thus suggests no significant rotations between localities. This is further supported by the lack of important regional deformation after emplacement of these flat-lying rocks. Given that no significant internal rotations can be identified, we further investigate the possibility of a wholesale regional rotation by comparing the overall VGP of the Moesian Platform and Bulgarian Rhodope to 20 Ma and 30 Ma poles from three existing APWPs of Eurasia (Fig. 5a). In all cases the rotation is not statistically significant at the 95% confidence level, thus precluding important wholesale regional rotation after the late Eocene–early Oligocene formation of these rocks.

An opportunity to expand our dataset is provided by the existence of published data from 15 paleomagnetic site-mean directions from upper Eocene–lower Oligocene volcanics located directly south of the Bulgarian Rhodope (nearby Thrace, across the border in northern Greece (Kissel et al., 1986a)). 10 out of these 15 sites are selected after applying our cut-off of $k<50$. These provide similar results to the one obtained in the present study (Fig. 5b). The 10 VGPs calculated are combined to our original 50-VGP dataset. After 4 VGPs are removed by the Vandamme (1994) cut-off, we derived an overall VGP

Please cite this article as: van Hinsbergen, D.J.J., et al., No significant post-Eocene rotation of the Moesian Platform and Rhodope (Bulgaria): Implications for the kinematic evolution of the Carpathian and Aegean arcs, Earth Planet. Sci. Lett. (2008), doi:10.1016/j.epsl.2008.06.051

Table 1
New and published paleomagnetic results of Eocene–Oligocene volcanic sites of the Moesian Platform and Rhodope

Locality						Tilt	Tilt Corrected					Tilt Corrected							Age
Lava/neck site	Lat	Lon	Type	Na	Nc	strike/dip	λ	ϕ	*k*	A95	Palat	D	ΔD	I	ΔI	*k*	α95	pol	Ma
New data																			
Suhindol				12	11		84.1	62.1	25.2	9.3	45.3	6.1	13.3	64.4	7.3			n/r	19.4–24.0 [43]
SU 1*	43.1681	25.1263	gc	8	6	000/00	83.0	126.9				189.2		−60.4				r	
SU 2*	43.1681	25.1263	gc	8	7	000/00	84.6	113.1				187.4		−61.9				r	
SU 3	43.1681	25.1263	gc	8	7	000/00	78.6	128.1				194.5		−58.9		896.6	2.0	r	
SU 4	43.1681	25.1263	gc	8	7	000/00						188.8		−56.5		44.2	9.2	r	
SU 5	43.2902	25.1736		8	7	000/00	65.9	156.9				19.7		43.5		141.1	5.1	n	
SU 6	43.2902	25.1736	gc	8	8	000/00	76.4	−155.2				0.1		48.7		75.5	6.4	n	
SU 7	43.2902	25.1736	gc	8	8	000/00	55.2	3.6				138.1		−80.6		987.2	1.8	r	
SU 8	43.2285	25.1526		8	8	000/00	80.5	34.3				2.5		69.1		205.2	4.2	n	
SU 9	43.2285	25.1526		8	8	000/00	77.8	55.5				10.3		69.6		193.2	4.0	n	
SU 10	43.2285	25.1526		8	8	000/00	73.9	76.6				20.5		68.4		66.3	6.9	n	
SU 11	43.2285	25.1526		8	7	000/00	80.4	−1.7				353.0		68.4		113.8	5.7	n	
SU 12	43.2285	25.1526	gc	8	6	000/00	74.1	−1.6				347.0		71.9		993.3	2.1	n	
Yabalkovo				12	12		72.5	28.1	45.1	6.5	58.9	181.5	12.7	−73.2	4.1			r	31.5–35.0 [27]
YA 1	42.0415	25.2345	gc	8	8	000/00	57.3	48.1				215.6		−79.1		181.2	4.1	r	
YA 2	42.0415	25.2345	gc	8	8	000/00	62.6	38.1				195.9		−78.6		215.0	3.8	r	
YA 3	42.0415	25.2345		8	8	000/00	77.7	20.0				178.1		−70.2		544.2	2.4	r	
YA 4	42.0415	25.2345	gc	8	7	000/00	67.0	45.7				197.3		−75.5		120.7	5.5	r	
YA 5	42.0446	25.2450	gc	8	8	254/05	71.6	17.2				174.9		−74.0		1975.7	1.2	r	
YA 6	42.0446	25.2450		8	7	254/05	73.0	−4.3				165.0		−71.4		370.2	3.1	r	
YA 7	42.0446	25.2450		8	7	254/05	55.9	16.5				160.7		−82.4		1283.6	1.7	r	
YA 8	42.0446	25.2450		8	7	254/05	73.2	−20.8				160.2		−68.8		313.5	3.1	r	
YA 9	42.0346	25.2773		8	8	000/00	70.3	32.5				185.1		−74.8		243.1	3.6	r	
YA 10	42.0346	25.2773		8	8	000/00	85.4	−25.4				175.0		−63.3		68.8	6.7	r	
YA 11	42.0346	25.2773		8	8	000/00	77.3	46.5				187.7		−69.8		53.9	7.6	r	
YA 12	42.0346	25.2773		8	8	000/00	79.1	86.5				193.9		−64.6		128.8	4.9	r	
Zvezdel				12	11		79.5	112.9	20.2	10.4	38.8	194.2	13.4	−58.1	9.6			r	31.0–33.0 [27]
ZV 1	41.2781	25.2499		9	9	000/00	72.0	165.1				192.9		−45.2		66.2	6.4	r	
ZV 2	41.2745	25.2493	gc	8	8	000/00	82.6	106.0				189.9		−61.0		328.6	3.1	r	
ZV 3	41.2727	25.2488		8	5	000/00	87.1	91.2				183.6		−61.3		153.0	6.2	r	
ZV 4	41.2712	25.2478	gc	8	8	000/00	68.2	175.1				191.6		−38.6		70.5	6.6	r	
ZV 5	41.2656	25.2511		8	8	000/00	86.2	78.3				184.2		−62.2		124.2	5.0	r	
ZV 6	41.2651	25.2509		8	8	000/00	72.6	178.1				188.7		−43.5		253.9	3.5	r	
ZV 7	41.2542	25.2561		8	–	000/00						–		–		–	–		
ZV 8	41.2539	25.2561		8	7	000/00	63.7	88.3				216.1		−65.7		219.9	4.1	r	
ZV 9	41.2471	25.2567		8	8	000/00	71.4	147.5				198.1		−48.9		82.7	6.1	r	
ZV 10	41.2469	25.2480	gc	8	7	000/00	58.8	119.4				217.7		−51.8		122.9	5.5	r	
ZV 11	41.2447	25.2473		9	9	324/15	63.0	37.1				193.9		−78.1		218.8	3.5	r	
ZV 12	41.2444	25.2466		8	8	324/15	66.4	9.3				165.8		−75.9		93.7	5.8	r	
Bratsigovo				4	3		66.4	140.9	35.4	21.0	30.7	204.1	24.6	−47.4	24.9			r	late Eo-Oligocene
BR 1	42.0175	24.2601	gc	8	8	224/20	75.7	177.4				187.3		−48.0		122.0	5.0	r	
BR 2	42.0173	24.2603		8	8	244/12	60.0	142.3				208.9		−41.5		201.1	3.9	r	
BR 3	42.0173	24.2603	gc	8	8	244/12	59.5	122.7				216.0		−50.7		3401.8	0.9	r	
BR 4	42.0169	24.2604	gc	8	8	244/12						236.8		−54.2		28.6	10.5	r	
Dospat				10	9		67.1	139.1	72.3	6.1	30.7	204.0	7.1	−47.4	7.2			r	late Eo-Oligocene
DO 1	41.4102	24.0940		8	8	000/00	74.9	116.8				199.6		−58.3		264.6	4.1	r	
DO 2	41.4102	24.0940		8	7	000/00	60.1	135.3				211.1		−44.3		220.3	4.1	r	
DO 3–5	41.4103	24.0922		16	16	000/00	69.0	134.6				203.3		−50.6		217.8	2.5	r	
DO 4	41.4104	24.0919		8	8	000/00	62.3	128.9				211.2		−48.8		163.8	4.3	r	
DO 6	41.4111	24.0917		8	8	000/00	63.9	151.0				202.5		−40.8		372.4	2.9	r	
DO 7	41.4131	24.0920		8	8	000/00	75.2	114.1				199.4		−59.0		94.8	5.7	r	
DO 8	41.4130	24.0912		8	7	000/00	74.8	175.7				188.1		−46.4		198.7	4.3	r	

(continued on next page)

Table 1 *(continued)*

Locality						Tilt	Tilt Corrected					Tilt Corrected							Age
Lava/neck site	Lat	Lon	Type	Na	Nc	strike/dip	λ	ϕ	*k*	A95	Palat	D	ΔD	I	ΔI	*k*	α95	pol	Ma
DO 9	41.4135	24.0878		8	8	000/00	59.3	139.8				210.2		−41.3		185.2	4.1	r	
DO 10	41.4138	24.0876		8	8	000/00	58.1	149.6				207.1		−35.1		147.3	4.6	r	
Banichan				8	4		75.3	286.6	7.1	37.2	32.5	160.5	45.8	−57.2	35.0			n/r	28–29 Ma [44]
BA 1	41.3862	23.4203	gc	8	6	000/00	89.4	15.7				179.9		−60.9		94.1	6.9	r	
BA 2	41.3857	23.4211		8	6	000/00	55.4	−75.9				140.4		−47.2		332.1	3.7	r	
BA 3	41.3854	23.4218		9	7	000/00	45.2	−59.4				124.1		−51.7		58.9	7.9	r	
BA 4	41.3854	23.4218		8	8	000/00						133.7		−61.2		31.9	10.0	r	
BA 5	41.3832	23.4240		8	5	000/00						162.2		−42.2		36.2	12.9	r	
BA 6	41.3820	23.4254		8	8	000/00						145.0		−49.3		37.5	9.2	r	
BA 7	41.3817	23.4354		8	5	000/00						141.2		−43.3		26.2	13.3	r	
BA 8	41.3807	23.4254	gc	8	8	054/15	67.8	130.9				25.1		51.1		221.3	3.7	n	
20 Ma pole				12	11		84.1	62.1	25.2	9.3	45.3	6.1	13.3	64.4	7.3			n/r	
30 Ma pole				39	37		79.9	101.7	18.3	5.7	43.2	13.5	7.8	61.9	4.7			n/r	
Combined pole				50	48		80.2	96.9	19.3	4.8	43.9	13.0	6.7	62.6	3.9			n/r	
* site average is a great circle: direction is determined comparing these great circles with the directions from this locality using the method of [50]																			
Previously published data																			
(Kissel et al. 1986a)																			
Thessaly (Greece)				15	9		75.5	157.5	80.6	5.8	30.7	12.5	6.7	50.0	6.5			n/r	late Eo-Oligocene
TH 297	41.1125	25.5353			10		73.7	154.4				194.6		−49.0		133.0	3.8	r	
TH 301	40.9012	25.5384			6		80.6	−167.6				2.5		51.0		52.0	8.0	n	
TH 307	40.9013	25.5402			9		84.2	135.8				7.0		58.0		302.0	2.7	n	
TH 300	40.8887	25.5479			8		79.0	−149.9				359.0		49.0		172.0	3.7	n	
TH 306	41.1061	25.5637			9							13.8		35.2		19.0	10.0	n	
TH 292	41.0998	25.8663			10		83.4	148.0				187.0		−56.8		52.0	6.0	r	
TH 296	41.2417	25.8883			9							189.9		−58.7		19.0	10.2	r	
TH 291	41.1566	25.8883			10		65.7	150.3				22.0		43.2		50.0	6.2	n	
TH 293	41.1250	25.9482			9							335.3		38.3		37.0	7.6	n	
TH 294	41.1755	25.9482			8							229.0		−45.5		10.0	15.4	r	
TH 290	40.9328	26.1752			6		70.2	144.9				200.0		−48.6		107.0	6.0	r	
TH 304	41.1534	26.2161			10							161.5		−27.5		31.0	7.8	r	
TH 289	40.9580	26.2192			10		70.9	151.1				197.8		−47.4		117.0	4.0	r	
TH 303	41.1597	26.2287			11		58.1	−120.7				162.8		−24.8		73.0	5.0	r	
TH 288	40.9832	26.2414			5		64.6	155.8				201.0		−40.0		84.0	6.8	r	
Eo-Oligocene pole																			
Combined pole				60	56		80.1	112.4	21.9	4.2	41.3	13.2	5.6	60.4	3.6			n/r	

Lat = latitude of the site; Lon = longitude of the site; Type indicates ‘gc’ when the site average was constructed using the great circle method of McFadden and McElhinny (1988); *N*a = number of samples analysed; *N*c = number of sampled used to construct the site average; Tilt: strike and dip applying the left hand rule; λ = longitude of the virtual geomagnetic pole (VGP); ϕ = latitude of the VGP; K = Fisher (1953) precision parameter for the average pole; A95 = 95% confidence limit of the average pole; Palat = paleolatitude; D = declination; ΔD = 95% confidence limit of the declination; I = inclination; ΔI = 95% confidence limit of the inclination; k = Fisher (1953) precision parameter for the average direction (in case of lava sites); α95 = 95% confidence limit of the average direction (in case of lava sites); pol = normal (*n*) or reverse (*r*) polarity.

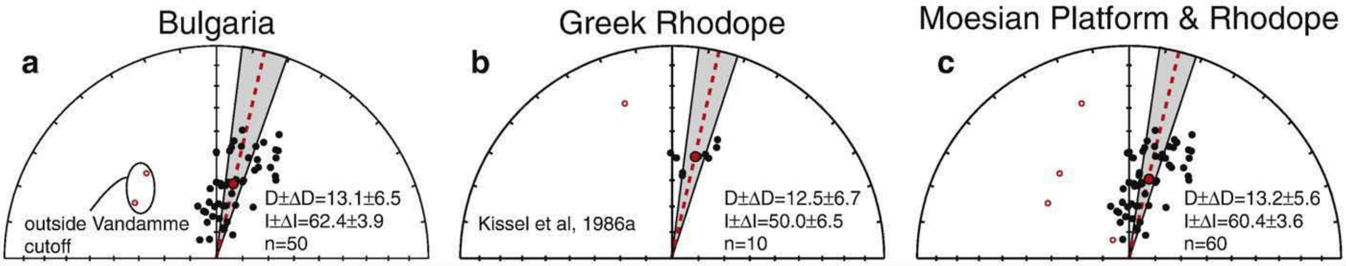

locality	n	*Besse & Courtillot (2002) reference direction (30 Ma)*				*Torsvik et al (2008) reference direction (30 Ma)*				*Schettino & Scotese (2004) reference direction (30 Ma)*			
Moesian platform/Rhodope		rotation	error	flattening	error	rotation	error	flattening	error	rotation	error	flattening	error
20 Ma pole	11	0.1	13.7	-5.9	7.7	0.1	13.9	-5.6	7.8	3.6	14.3	-7.2	8.3
30 Ma pole (Bulg. + Greece)	46	6.9	9.1	-6.0	6.0	6.2	9.1	-5.5	6.0	9.9	12.8	-6.1	9.2
all	56	6.6	7.3	-4.5	5.2	5.9	6.6	-4.0	4.5	9.6	11.5	-4.6	8.7

Fig. 5. Equal-area projections for the Bulgarian data (a), the northern Greek data of Kissel et al. (1986a) (b) and the combination of all available data from the upper Eocene and Oligocene of the Moesian Platform and Rhodope (c). All data have been plotted as normal directions. Data and statistical parameters are given in Table 1. D = declination, I = inclination, ΔD = 95% confidence limit in declination, ΔI = 95% confidence limit in inclination, n = number of lava sites. Data from the Greek Rhodope were previously published by Kissel et al. (1986a). D: Comparison of our new Eocene–Oligocene average direction for the Moesian Platform and Rhodope with reference directions at 30 Ma obtained from the apparent polar wander paths of Besse and Courtillot (2002), Schettino and Scotese (2005) and Torsvik et al. (in press). Poles are translated to directions at the coordinate 41.56°N/25.33°E.

(n = 56; λ = 80.1°N; φ = 112.4°E; A_{95} = 4.2°; K = 21.9; Scatter = 15.6), yielding D ± ΔD/I ± ΔI of 13.2 ± 5.6/60.4 ± 3.6 (Fig. 5c). This result compares well with the 14.5° declination previously published for five lower Oligocene lavas in the Greek Rhodope (Atzemoglou et al., 1994), however, as the latter publication does not report the lava site-means, we cannot incorporate these results in our average. When compared to the Eurasian APWPs, our data expanded with the Greek Rhodope data also indicate no statistically significant regional rotation (Fig. 5). We therefore conclude that the Moesian Platform and Rhodope can be considered to be stable entities when compared in the kinematic reconstructions, to the large rotations in the Aegean and Carpathian domains since ~30 Ma.

5. Regional kinematic implications

5.1. Implications for the Moesian Platform and Rhodope

The majority of the previous paleomagnetic results obtained from the Moesian Platform (Dolapchieva, 1994) and overlying nappes of the Balkanides have been obtained from pre-Cenozoic units. Analyses in middle Triassic and Jurassic rocks from the Balkanides generally show no deviation from the Eurasian directions (Kruczyk et al., 1988; Muttoni et al., 2000). In some places, however, remagnetization has been identified: South of the Moesian Platform, (Kruczyk et al., 1990) sampled Jurassic sediments from the Srednogorie zone which were remagnetized, possibly in the late Cretaceous. Jordanova et al. (2001) concluded that sites in the Triassic to Cretaceous from the Balkanides of western Bulgaria were remagnetized based on negative fold tests in these sediments. Based on the best fit of the remagnetized directions with comparison with the Eurasian APWP, the age of this remagnetization could be Eocene, which would imply a ~15° clockwise rotation of the Balkanides. Jordanova et al. (2001) suggested that these rotations are local and associated with the last compressional phases that affected the Balkanides in the middle Eocene. This is a possible scenario, given that we find neither significant post-Eocene rotation, nor evidence for a post-Eocene remagnetization. Together with our results, the paleomagnetic data from the Moesian platform indicates that some local rotations (~15° clockwise) may have occurred during Eocene compression but that after this time, no significant rotation affected the Moesian Platform and the Rhodope region.

5.2. Implications for the Carpathian arc

Kinematic reconstructions of the evolution of the Carpathian arc are based on quantitative constraints mostly from structural geology data and vertical-axis block rotations inferred from paleomagnetic studies (e.g. Balla, 1987; Linzer, 1996; Zweigel et al., 1998; Csontos and Voros, 2004). Two distinctive tectonic domains separated by the mid-Hungarian deformed belt (Csontos and Nagymarosy, 1998) have been defined: the northwestern Carpatho–Pannonian domain (the Alcapa block) with systematic counterclockwise rotations and the south-eastern Carpatho–Pannonian domain (the Tisza block) with systematic clockwise rotations (Fig. 1). Based on existing kinematic reconstructions, the motion of Tisza was roughly coeval with the rotation and emplacement of the Alcapa block (following Ustaszewski et al. (in press), we infer a minimum amount of ~25° of counter-clockwise rotation of the Alcapa block since the middle Miocene). These reconstructions assume the Moesian Platform to have formed a stable promontory during the motion of the Tisza block. First, northward motion of Tisza along the western edge of the Moesian Platform is evidenced by late Cretaceous nappe stacking followed by arc-parallel extension dated late Eocene–Oligocene by thermochronology (e.g. Schmid et al., 1998; Fügenschuh and Schmid, 2005). Secondly, the Tisza block—driven by eastward roll-back of the Carpathian slab and northward motion of Apulia—rotated clockwise around the northwestern corner of the Moesian Platform and translated eastward into the Carpathian embayment (Balla, 1987; Sperner et al., 2002; Csontos and Voros, 2004). The timing of this second phase is still controversial because of discrepancies between structural geology data and the age of teconic rotations derived from paleomagnetism (Patrascu et al., 1994; Fügenschuh and Schmid, 2005).

We review here briefly the available paleomagnetic data pertaining to the rotation of the Tisza block, adding data from Cretaceous rocks to the existing review of Dupont-Nivet et al. (2005; see Appendix A). In reviewing the data, we have attempted to exclude results superseded by more reliable paleomagnetic data and/or better age control from the same location. In particular, published results from the Apuseni Mountains with an Eocene–Oligocene age (Patrascu et al., 1994) that are commonly used for kinematic reconstructions (Schmid et al., 1998; Fügenschuh and Schmid, 2005) have been found to be of Maastrichian age (Panaiotu, 1998). When compared to the Eurasian APWP, our review shows that the mean post-Cretaceous clockwise rotation (79.1 ± 9.6°) is indistinguishable from the mean Eocene–Oligocene clockwise rotation (72.2 ± 16.6°) suggesting that no significant rotation can be demonstrated between Cretaceous and Oligocene time and that most of the eastward motion and rotation of Tisza occurred after the Oligocene. The mean post-Eocene–Oligocene data can be directly compared to the reference pole of the Moesian Platform derived from the present study to derive a 68.4 ± 16.7° post-

Oligocene clockwise rotation of Tisza with respect to the Moesian Platform. This rotation is statistically indistinguishable—albeit higher—from the structurally constrained 53° clockwise rotation prediction of Schmid et al. (1998). This prediction is required by (1) the accommodation of 140 km of shortening between the Tisza Block and the East European cratonic margin and (2) the reconstruction of a pivot point for the Tisza block rotation from the arcuate shape of the nortwestern edge of the Moesian Platform (i.e. the curved Timok and Cerna–Jiu fault and associated structures (Fig. 1)). The slightly higher paleomagnetic rotation compared to this prediction may result from the 140 km shortening being an underestimation, the defined pivot point being too far from the Tisza block or, more likely, overestimation of the block rotation as a result of additional clockwise rotations due to local dextral shear associated with the emplacement of the Tisza block. For the Miocene rotation results, it is necessary to distinguish between data of the Tisza block proper (mostly from the Apuseni Mountains and the Transylvania Basin, Fig. 1) from the Southern Carpathians data on the margin of the Tisza block. Indeed, middle Miocene data from foreland deposits of the Southern Carpathians revealed systematic post-13 Ma clockwise rotations (average of 31.6±6.7°, see Appendix A) interpreted as local rotations due to distributed dextral shear during eastward motion of the Tisza block into the Carpathian embayment (Dupont-Nivet et al., 2005). This suggests distributed dextral shear within the Southern Carpathian belt and supports that this mechanism accommodated the dextral motion without the occurrence of major surface strike-slip faults along the Southern Carpathians as previously suggested (Fügenschuh and Schmid, 2005). The absence of significant rotation in rocks younger than ~6 Ma along the Southern Carpathians suggest that the dextral motion of the Tisza block occurred between ~13 and ~6 Ma, in good agreement with basin analysis data (Bertotti et al., 2003; Matenco et al., 2003). A set of data from the Tisza block proper (Apuseni Mountains and Transylvania Basin) provides a remarkable progressive record during the clockwise rotation between roughly 15 and 10 Ma (Panaiotu, 1998, 1999). Allowing that this set of data is representative for the entire Tisza block, it indicates that most if not all of the rotation occurred in this short time frame. In light of our results showing the post-Eocene stability of the Moesian Platform, we confirm that the Tisza rotation can be fully attributed to the emplacement of the Tisza block around the Moesian Platform with associated dextral shear along its western and northern margin. In addition, the fact that the Moesian Platform has not rotated together with the Tisza block at this time, implies that the coeval southward migration and rotation of the Aegean arc did not include the Moesian Platform, and should be accommodated within the Aegean region.

5.3. Implications for the Aegean arc

A 600-km long region stretching from northern Albania over mainland western Greece to the Peloponnesos underwent approximately 50° clockwise rotation (e.g. Horner and Freeman, 1983; Kissel and Laj, 1988; Morris, 1995; Speranza et al., 1995; van Hinsbergen et al., 2005a). This region is bounded to the north by the Scutari–Pec transform fault (Fig. 1), north of which, in the Dinarides, no Cenozoic rotations occurred (Kissel et al., 1995). The youngest rocks which experienced this amount or rotation include the upper Burdigalian of the Klematia–Paramythia basin in western Greece (with an age as young as ~17 Ma (van Hinsbergen et al., 2005c)) and volcanic rocks on Evia of 15 and 13 Ma (Kissel et al., 1986b; Morris, 1995), leading van Hinsbergen et al. (2005a) to argue that the majority of clockwise rotation occurred after 15 Ma. Rocks of 8 Ma and younger in the Florina–Ptolemais–Lava basin in northern Greece, as well as on Corfu experienced no more than 10° clockwise rotation (van Hinsbergen et al., 2005a), suggesting that the bulk of the west Aegean rotation occurred between 15 and 8 Ma.

Several lines of evidence suggest that this region can be considered as a single rotating block. The western Aegean region displays a series of nappes which are internally folded. The strike of these folds is proportional to the amount of rotation (Horner and Freeman, 1983; van Hinsbergen et al., 2005a) and provides a clear structural grain showing little post-folding deformation of the region. Local rotations remain confined along discrete fault zones such as the Gulf of Corinth and the Thesprotiko shear zone (van Hinsbergen et al., 2006). This, in combination with the very consistent amount of rotation all over this region, led Kissel and Laj (1988) and van Hinsbergen et al. (2005a) to conclude that this region can be considered as a single rotating block, with little internal fragmentation.

Our new reference direction for the Moesian Platform and Rhodope allows us to accurately quantify the rotation difference between western Greece and the Rhodope, which is critical to evaluate kinematic models for the Aegean region. However, for western Greece Kissel and Laj (1988) and van Hinsbergen et al. (2005a) mention 'approximately 50°' of rotation, but do not give statistical values for this average. Therefore, we calculated the average declination and inclination from all published sites obtained from the Oligocene of western Greece and Albania. Ninety site-mean directions remain after discarding locally-rotated sites in central Greece and the northern Peloponnesos, following van Hinsbergen et al. (2005a). The average given in Table 2 (D±ΔD/I±ΔI of 51.2±5.6/34.7±6.5) is based on 85 site-mean directions, (five were excluded by the Vandamme (1994) cut-off: see Appendix A). The outcome of the parametric reversals test of Tauxe (1998) on these data is positive with 95% confidence. The inclination error is very large, which can be straightforwardly explained by inclination shallowing due to compaction in these sediments. This result compared to our newly obtained direction for the Moesian Platform yields a 38.0±7.2° clockwise rotation difference between western Greece and the Moesian Platform/Bulgarian Rhodope (Table 2).

Kissel and Laj (1988) and Kissel et al. (2003) argued that the pivot point of the rotation was located at the northwestern tip of the west Aegean domain in northern Albania at the Scutari–Pec transform fault (Fig. 1). However, 38.0±7.2° clockwise rotation difference between the west-Aegean domain and the Moesian Platform around this pivot point would require 265±50 km of N–S to NE–SW extension in the Aegean back-arc at the latitude of the Gulf of Corinth, 400 km away from northern Albania. The total amount of N–S extension in the

Table 2
Oligocene direction for the west-Aegean domain, and comparison of the declination with our new reference direction for the Moesian Platform and Rhodope

Locality	Reference direction					Pole			Direction						Age
	lat	lon	n	n (vD)	λ	ϕ	κ	A95	palat	D	ΔD	I	ΔI	pol	Ma
West Aegean	38.15	21.44	90	85	58.8	197.7	13.6	4.3	19.1	51.2	4.6	34.7	6.5	n/r	23–33
Moesian Platform	41.56	25.33	60	56	80.1	112.4	21.9	4.2	41.3	13.2	5.6	60.4	3.6	n/r	20–37
Rotation difference										38.0	7.2				

The inclination in the west Aegean domain is very low with respect to the expected inclination, which can be straightforwardly explained by inclination shallowing due to sedimentary compaction. Data used to construct the new west-Aegean paleomagnetic direction for the Oligocene are given in online Appendix B. See caption of Table 1 for explanation of abbreviations in the table header. n=number of sites; n (vD): amount of sites used for calculation of poles and directions after the Vandamme (1994) cut-off.

Please cite this article as: van Hinsbergen, D.J.J., et al., No significant post-Eocene rotation of the Moesian Platform and Rhodope (Bulgaria): Implications for the kinematic evolution of the Carpathian and Aegean arcs, Earth Planet. Sci. Lett. (2008), doi:10.1016/j.epsl.2008.06.051

Aegean region since approximately 25 Ma was calculated at approximately 300–400 km (Gautier et al., 1999; Jolivet, 2001). Much of this extension, however, was accommodated by formation of metamorphic core complexes, which occurred for a large part prior to 15 Ma (Jolivet, 2001). Moreover, this amount includes up to 100 km of extension accommodated on Crete and in the Sea of Crete (Ring et al., 2001), which lie south of the rotating domain. Thus, the amount of extension required by a rotation with a pivot point in northern Albania is by no means in line with the Aegean reconstructions. This is not to say that there was no extension at all. The Strimon detachment in the Greek Rhodope was active after 15 Ma (Dinter and Royden, 1993; Sokoutis et al., 1993; Brun and Sokoutis, 2007; see discussion below) and additional exhumation and extension occurred in that time in eastern central Greece (Lacassin et al., 2007). Although precise extension estimates on these structures are still scarce, the total amount of post-15 Ma extension in this region is unlikely to be much more than 150 km. We thus conclude that the pivot point of the western Aegean rotations cannot have been positioned in northern Albania, but was more likely placed within the rotating domain itself. Given the uncertainties in estimating the amount and distribution of post-15 Ma extension in Greece it is not possible to determine the location of the pivot point with certainty, but several lines of argumentation lead us to postulate its location on a meridian line located on the western margin of the Moesian Platform, around the longitude of Mt Olympos, i.e. ~22.50°E (Figs. 1 and 6). Firstly, no important middle to late Miocene NE–SW extension occurred west of this line, even though there is a rotation difference to be accommodated between Albania and the eastern Balkanides/Moesian Platform. Secondly, the geodynamics of the Aegean region make this location likely: east of this line, the African slab has been (and likely still is) rolling back south(west)ward, whereas west of this line, the motion of Apulia was continuously northward together with Africa (Besse and Courtillot, 2002; Govers and Wortel, 2005). Within this geodynamic framework, rotation of the west-Aegean domain about a pivot point located on this line would be a likely consequence.

This is in line with a pivot point position proposed by Brun and Sokoutis (2007) based on the independent study of the Eocene to Miocene Southern Rhodope Core Complex (Fig. 1). This triangular core complex developed in two stages, in a dome-in-a-dome sense, comparable to the Menderes core complex of western Turkey (Gessner et al., 2001). The first dome evolved since ~40 Ma, the second one cooled below ~300 °C since 15 Ma. Lineations within this core complex display a gradual ~20° trend change. A paleomagnetically determined ~20° clockwise rotation difference between the Chalkidiki peninsula and the Bulgarian Rhodope (Kondopoulou and Westphal, 1986) suggests the core complex formed during this rotation (with the new Bulgarian Rhodope reference direction obtained here, the data of for the Chalkidiki Peninsula since late Eocene–early Oligocene times ($D\pm\Delta D$ / $I\pm\Delta I=31.1\pm11.6/37.1\pm15.3$; Appendix A) yields a similar clockwise rotation difference across the Southern Rhodope Core Complex of 17.9±12.6° (Table 2)). However, Brun and Sokoutis (2007) suggest that the rotation occurred continuously since ~40 Ma which is at odds with the interpretation of van Hinsbergen et al. (2005b) who suggested that the rotation of the Chalkidiki peninsula occurred as part of the rotation of the west

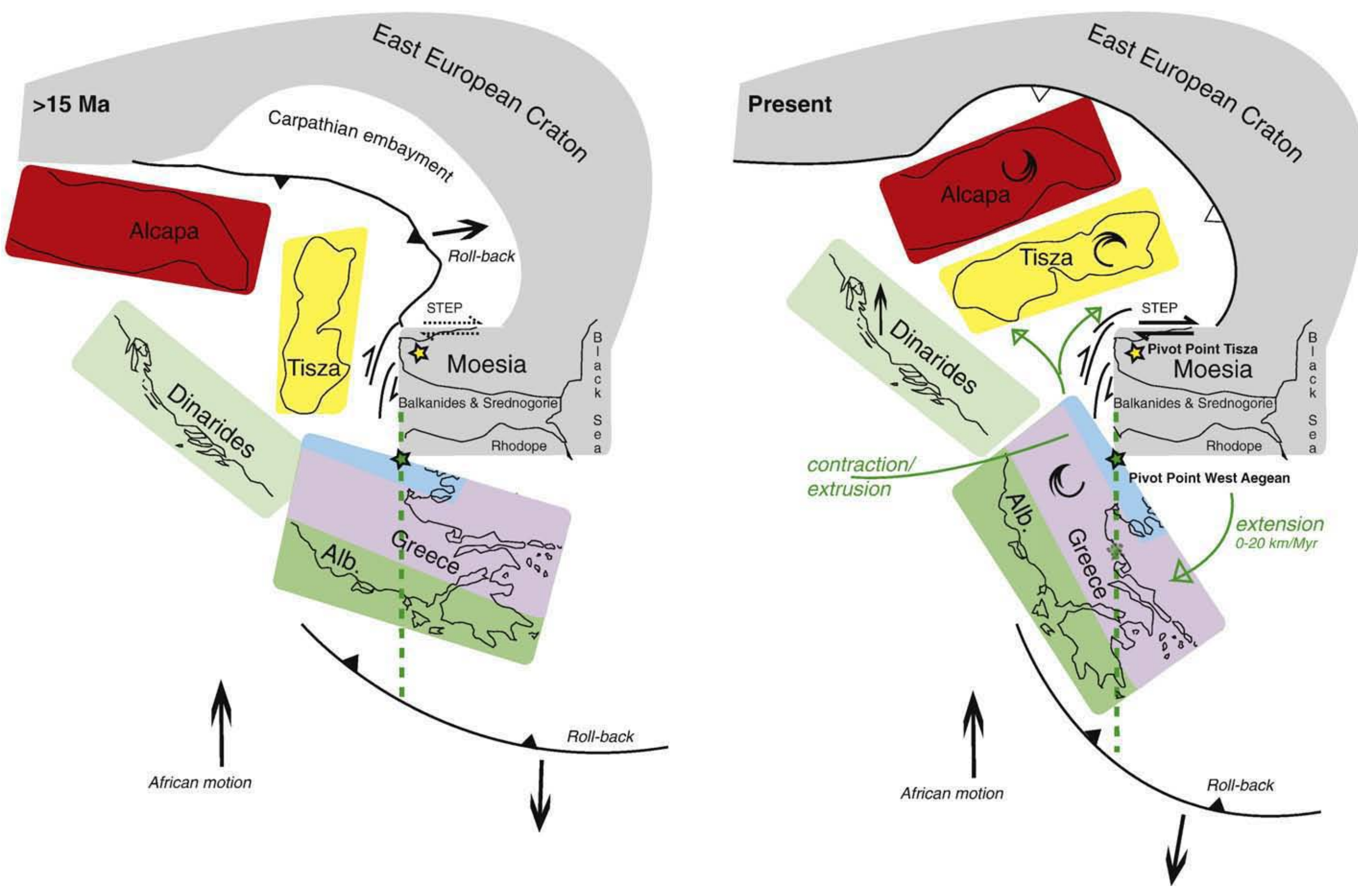

Fig. 6. Tentative scenario placing the (middle) Miocene west Aegean and southern Carpathian rotations in a kinematic and geodynamic context. We propose that rotation of the west-Aegean domain had a pivot point in the centre of the rotating domain due south of the western limit of the Moesian Platform. To the east, rotation was accommodated by (roll-back-related) extension in the Aegean back-arc. To the west, rotation was accommodated by escape of the Tisza block into the Carpathian back-arc, triggered by eastward roll-back of the Carpathian subduction zone, and coeval rotations along the northern edge of the Moesian Platform related to activity of the south Carpathian STEP fault (Dupont-Nivet et al., 2005; Govers and Wortel, 2005). Rotation of the Alcapa Block and the reconstruction of the Carpathian Embayment are taken from Ustaszewski et al. (in press).

Please cite this article as: van Hinsbergen, D.J.J., et al., No significant post-Eocene rotation of the Moesian Platform and Rhodope (Bulgaria): Implications for the kinematic evolution of the Carpathian and Aegean arcs, Earth Planet. Sci. Lett. (2008), doi:10.1016/j.epsl.2008.06.051

Aegean region after 15 Ma. The (sub-)Pelagonian nappe of eastern mainlaind Greece revealed no rotation between Eocene and early Miocene times in the Mesohellenic basin (van Hinsbergen et al., 2005b), whereas this nappe already accreted to the overriding plate—including the Rhodope—before the Eocene (Ricou et al., 1998; van Hinsbergen et al., 2005a). In addition, there is no structural evidence for deformation that may have accommodated a rotation difference between the Pelagonian zone of mainland Greece and the Chalkidiki peninsula before the post-15 Ma rotation of western Greece. A possible scenario satisfying both the timing of rotation and the 20° change in lineation trends is that the first dome of the Southern Rhodope Core Complex formed without rotation of the Chalikidiki peninsula with respect to the northern Rhodope and the second dome formed in response to the ~20° rotation since ~15 Ma.

The finite rotation of the west-Aegean domain is however ~20° more than Chalkidiki suggesting the west Aegean pivot point may have started at the northwestern tip of the southern Rhodope core complex, as proposed by Brun and Sokoutis (2007), but then moved southward through time, either gradually or suddenly.

Extension rates implied by a pivot point halfway the rotating domain as indicated in Fig. 6 would increase from the pivot point eastward from 0 to a maximum of ~20 km/Myr (assuming the Aegean block east of the pivot point is ~250 km long and rotated ~30° clockwise with respect to the Bulgarian Rhodope between 15 and 8 Ma; the final 10° occurring after 8 Ma (van Hinsbergen et al., 2005b)). This is in reasonable agreement with average extension rates estimated for the last ~30 Ma in the Aegean system of Gautier et al. (1999) and Jolivet (2001) of ~10–15 km/Myr.

5.4. Kinematic link between Aegean and Carpathians?

Using this new pivot point has interesting tectonic and kinematic implications. The rotation of the Aegean domain northwest of the pivot point in central Greece postulated above requires well over 100 km NE–SW convergence between Albania and the western Moesian Platform. This convergence may have been accommodated by compressional deformation and/or northward extrusion of a wedge of material in between these regions (Fig. 6). On the one hand, compressional deformation is supported by regional geological features of this region. The Albanian equivalents of the Tripolitza and especially Pindos nappes have been largely overthrusted by the Vardar ophiolites, thus suggesting a larger amount of convergence than in Greece. On the other hand, extrusion may have been associated to the northward extrusion and clockwise rotation of the Tisza block around the northwestern edge of the Moesian Platform (Dupont-Nivet et al., 2005). We favor this scenario supported by the coincidence of the Tisza block emplacement with the Aegean rotations (van Hinsbergen et al., 2005a). However, extrusion requires coeval strike-slip motions on either side of the wedge that remain to be identified in the field, and the larger Albanian shortening remains to be quantified and dated. Clearly, further work is required to test these hypotheses, but the tentative reconstruction we propose provides the best fit for the kinematic and rotation information available for the Aegean and Carpathian regions.

6. Conclusion

Kinematic reconstructions for the Carpathian and Aegean arcs, loci of development of fundamental models for mountain building, orogenic collapse and geodynamics, generally assume the Moesian Platform, located in the core of the Carpathian–Balkan arc and the southern Rhodope Mountains, to be stably attached to the East European craton during the Cenozoic. In this paper we provide a new paleomagnetic reference direction ($D \pm \Delta D / I \pm \Delta I = 13.2 \pm 5.6 / 60.4 \pm 3.6$), which confirms this assumption: there is no significant deviation of the Eocene–Oligocene declination of the Moesian platform and Rhodope with respect to published contemporaneous European apparent polar wander paths.

This new reference point has important implications for the regional kinematic evolution of the south-eastern European region. We reviewed paleomagnetic results obtained from the Tisza Block which rotated around the northwestern margin of the Moesian platform during its post-Eocene emplacement into the Carpathian back-arc. The Tisza block underwent 68.4 ± 16.7° of clockwise rotation with respect to the Moesian platform during the middle Miocene (~15–10 Ma). This result is statistically indistinguishable from estimates derived from structural geology (Schmid et al., 1998). In addition, our finding confirms that the eastward emplacement of the Tisza block into the Carpathian back-arc was associated with dextral shear along the southern margin expressed by systematic clockwise rotations between 13 and 9 Ma in the Southern Carpathians foreland (Dupont-Nivet et al., 2005).

The new Eocene–Oligocene reference direction for the Moesian platform and Rhodope allows to accurately quantify the rotation difference with the west Aegean domain. We reviewed and recalculated the post-Oligocene rotation difference (which was largely accommodated between 15 and 8 Ma) at 38.0 ± 7.2°. Classically, the west-Aegean rotation is considered to occur around a pivot point located on the northwestern tip of the rotating domain, in northern Albania (Kissel and Laj, 1988). This would, however, imply that the west-Aegean rotation is entirely accommodated in the Aegean back-arc, requiring 265 ± 50 km of extension between the Moesian platform and the Gulf of Corinth. Aegean extension largely occurred prior to 15 Ma, and it is unlikely that more than 150 km of extension occurred in the Aegean back-arc during the west-Aegean rotation. We therefore propose that the pivot point of the west-Aegean rotation was located approximately in the middle of the rotating domain on the meridian line of the western margin of the Moesian platform, with extension to its east.

This new scenario predicts that material should be contracted or extruded in between northern Albania and the Moesian platform. This prediction is in line with the contemporaneous evolution of the Tisza block, rotating around the Moesian platform and into the Carpathian back-arc. We therefore postulate that the west-Aegean rotation is kinematically balanced by a combination of Aegean back-arc extension and the motion of the Tisza Block around the northwestern edge of the Moesian platform.

Acknowledgements

This study was carried out within the context of the Netherlands Research School of Integrated Solid Earth Sciences (ISES). DJJvH and GDN are funded through VENI grants of the Netherlands Organisation for Scientific research (NWO). CP was partially founded through CNCSIS grant 974. We thank Andy Biggin for rock magnetic discussions. Stefan Schmid and Kamil Ustaszewski are thanked for inspiring discussions and a preprint of their recent work on the Carpathian system. We appreciated constructive reviews by Laurent Jolivet and Giovanni Muttoni.

Appendix A. Supplementary data

Supplementary data associated with this article can be found, in the online version, at doi:10.1016/j.epsl.2008.06.051.

References

Atzemoglou, A., Kondopoulou, D., Papamarinopoulos, S., Dimitriadis, S., 1994. Paleomagnetic evidence for block rotations in the Western Greek Rhodope. Geophys. J. Int. 118, 221–230.

Balla, Z., 1987. Tertiary paleomagnetic data for the Carpatho-Pannonian region in the light of Miocene rotation kinematics. Tectonophysics 139, 67–98.

Bertotti, G., Matenco, L., Cloetingh, S., 2003. Vertical movements in and around the south–east Carpathian foredeep: lithospheric memory and stress field control. Terra Nova 15, 299–305.

Besse, J., Courtillot, V., 2002. Apparent and true polar wander and the geometry of the geomagnetic field over the last 200 Myr. J. Geophys. Res. 107, 2300 doi:10.1029/2000JB000050.

Biggin, A., Perrin, M., Dekkers, M.J., 2007. A reliable absolute palaeointensity determination obtained from a non-ideal recorder. Earth Planet. Sci. Lett. 257, 545–563.

Boccaletti, M., Manetti, P., Peccerillo, A., 1974. The Balkanides as an instance of back-arc thrust belt: Possible relation with the Hellenids. Geol. Soc. Amer. Bull. 85, 1077–1084.

Brun, J.-P., Sokoutis, D., 2007. Kinematics of the Southern Rhodope Core Complex (Northern Greece). Int. J. Earth Sci. 96, 1079–1099.

Burchfiel, B.C., Nakov, R., Tzankov, T., 2003. Evidence from the Mesta half-graben, SW Bulgaria, for the Late Eocene beginning of Aegean extension in the Central Balkan Peninsula. Tectonophysics 375, 61–76.

Butler, R.F., 1992. Paleomagnetism: Magnetic Domains to Geologic Terranes. Blackwell Scientific Publications, Boston. 195 p.

Cloetingh, S., Burov, E., Matenco, L., Toussaint, G., Bertotti, G., Andriessen, P.A.M., Wortel, M.J.R., Spakman, W., 2004. Thermo-mechanical controls on the mode of continental collision in the SE Carpathians (Romania). Earth Planet. Sci. Lett. 218, 57–76.

Csontos, L., Nagymarosy, A., 1998. The Mid-Hungarian line: a zone of repeated tectonic inversions. Tectonophysics 297, 51–71.

Csontos, L., Voros, A., 2004. Mesozoic plate tectonic reconstruction of the Carpathian region. Palaeogeogr. Palaeoclimatol. Palaeoecol. 210, 1–56.

Dimitriadis, S., Kondopoulou, D., Atzemoglou, A., 1998. Dextral rotations and tectonomagmatic evolution of the southern Rhodope and adjacent regions (Greece). Tectonophysics 299, 159–173.

Dinter, D., Royden, L., 1993. Late Cenozoic extension in northeastern Greece: Strymon Valley detachment system and Rhodope metamorphic core complex. Geol. Soc. Amer. Bull. 21, 45–48.

Dolapchieva, M., 1994. Review and taxonomy of data and results of the paleomagnetic investigation in Bulgaria performed by senior researcher Peter Nozharov and his team. Bulg. Geophys. J. 22, 40–50 (in Bulgarian with English summary).

Dunlop, D., Özdemir, Ö., 1997. Rock Magnetism: Fundamentals and Frontiers. Cambridge University Press, Cambridge. 573 p.

Dupont-Nivet, G., Vasiliev, I., Langereis, C.G., Krijgsman, W., Panaiotu, C., 2005. Neogene tectonic evolution of the southern and eastern Carpathians constrained by paleomagnetism. Earth Planet. Sci. Lett. 236, 374–387.

Fisher, R.A., 1953. Dispersion on a sphere. Proc. R. Soc. Lond. A217, 295–305.

Fügenschuh, B., Schmid, S.M., 2005. Age and significance of core complex formation in a very curved orogen: evidence from fission track studies in the South Carpathians (Romania). Tectonophysics 404, 33–53.

Gautier, P., Brun, J.-P., Moriceau, R., Sokoutis, D., Martinod, J., Jolivet, L., 1999. Timing, kinematics and cause of Aegean extension: a scenario based on a comparison with simple analogue experiments. Tectonophysics 315, 31–72.

Gessner, K., Ring, U., Johnson, C., Hetzel, R., Passchier, C.W., Güngör, T., 2001. An active bivergent rolling-hinge detachment system: Central Menderes metamorphic core complex in western Turkey. Geology 29, 611–614.

Govers, R., Wortel, M.J.R., 2005. Lithosphere tearing at STEP faults: response to edges of subduction zones. Earth Planet. Sci. Lett. 236, 505–523.

Horner, F., Freeman, R., 1983. Palaeomagnetic evidence from Pelagic limestones for clockwise rotation of the Ionian zone, Western Greece. Tectonophysics 98, 11–27.

Innocenti, F., Kolios, N., Manetti, P., Mazzuoli, R., Peccerillo, G., Rita, F., Villari, L., 1984. Evolution and geodynamic significance of the Tertiary orogenic volcanism in Northeastern Greece. Bull. Volcanol. 47, 25–37.

Jolivet, L., 2001. A comparison of geodetic and finite strain pattern in the Aegean, geodynamic implications. Earth Planet. Sci. Lett. 187, 95–104.

Jordanova, N., Henry, B., Jordanova, D., Ivanov, Z., Dimov, D., Bergerat, F., 2001. Paleomagnetism in northwestern Bulgaria: geological implications of widespread remagnetization. Tectonophysics 343, 79–92.

Kirschvink, J.L., 1980. The least-squares line and plane and the analysis of palaeomagnetic data. Geophys. J. R. Astrol. Soc. 62, 699–718.

Kissel, C., Laj, C., 1988. The tertiary geodynamical evolution of the Aegean arc: a paleomagnetic reconstruction. Tectonophysics 146, 183–201.

Kissel, C., Kondopoulou, D.P., Laj, C., Papadopoulos, P., 1986a. New paleomagnetic data from Oligocene formations of Northen Aegea. Geophys. Res. Lett. 13, 1039–1042.

Kissel, C., Laj, C., Mazaud, A., 1986b. First paleomagnetic results from Neogene formations in Evia, Skyros and the Volos region and the deformation of Central Aegea. Geophys. Res. Lett. 13, 1446–1449.

Kissel, C., Speranza, F., Milicevic, V., 1995. Paleomagnetism of external southern Dinarides and northern Albanides: implications for the Cenozoic activity of the Scutari-Pec shear zone. J. Geophys. Res. 100, 14999–15007.

Kissel, C., Laj, C., Poisson, A., Görür, N., 2003. Paleomagnetic reconstruction of the Cenozoic evolution of the Eastern Mediterranean. Tectonophysics 362, 199–217.

Kondopoulou, D., Westphal, M., 1986. Paleomagnetism of the Tertiary intrusives from Chalkidiki (northern Greece). J. Geophys. 59, 62–66.

Krohe, A., Mposkos, E., 2002. Multiple generations of extensional detachments in the Rhodope Mountains (northern Greece): evidence of episodic exhumation of high-pressure rocks. In: Blundell, D.J., Neubauer, F., Von Quadt, A. (Eds.), The Timing and Location of Major Ora Depositions in an Evolving Orogen. Geol. Soc. Lond. Spec. Publ., vol. 204, pp. 151–178.

Kruczyk, J., Kadzialko-Hofmokl, M., Nozharov, P., Petkov, N., Nachev, I., 1988. Paleomagnetism of Jurassic sediments from Balkan, Bulgaria. Acta Geophys. Pol. 36, 49–62.

Kruczyk, J., Kadzialko-Hofmokl, M., Nozharov, P., Petkov, N., Nachev, I., 1990. Paleomagnetic studies on sedimentary Jurassic rocks from southern Bulgaria. Phys. Earth Planet. Inter. 62, 82–96.

Lacassin, R., Arnaud, N., Leloup, P.H., Armijo, R., Meijer, B., 2007. Exhumation of metamorphic rocks in N Aegean: the path from shortening to extension and extrusion. eEarth 2, 1–35.

Lilov, P., Yanev, Y., Marchev, P., 1987. K/Ar dating of the Eastern Rhodope Paleogene magmatism. Geol. Balc. 17, 49–58.

Linzer, H.-G., 1996. Kinematics of retreating subduction along the Carpathian arc, Romania. Geology 24, 167–170.

Linzer, H.-G., Frisch, W., Zweigel, P., Girbacea, R., Hann, H.-P., Moser, F., 1998. Kinematic evolution of the Romanian Carpathians. Tectonophysics 297, 133–156.

Matenco, L., Bertotti, G., 2000. Tertiary tectonic evolution of the external East Carpathians (Romania). Tectonophysics 316, 255–286.

Matenco, L., Bertotti, G., Cloeting, S., Dinu, C., 2003. Subsidence analysis and tectonic evolution of the external Carpathian–Moesian Platform region during Neogene times. Sediment. Geol. 156, 71–94.

McFadden, P.L., Lowes, F.J., 1981. The discrimination of mean directions drawn from Fisher distributions. Geophys. J. R. Astrol. Soc. 67, 19–33.

McFadden, P.L., McElhinny, M.W., 1988. The combined analysis of remagnetisation circles and direct observations in paleomagnetism. Earth Planet. Sci. Lett. 87, 161–172.

McFadden, P.L., Merril, R.T., McElhinny, M.W., Lee, S., 1991. Reversals of the Earth's magnetic field and temporal variations of the dynamo families. J. Geophys. Res. 96, 3923–3933.

Morley, C.K., 1996. Models for relative motion of crustal blocks within the Carpathian region, based on restorations of the outer Carpathian thrust sheets. Tectonics 15, 885–904.

Morris, A., 1995. Rotational deformation during Palaeogene thrusting and basin closure in eastern central Greece: palaeomagnetic evidence from Mesozoic carbonates. Geophys. J. Int. 121, 827–847.

Muttoni, G., Gaetani, M., Budurov, K., Zagorchev, I., Trifonova, E., Ivanova, D., Petrounova, L., Lowrie, W., 2000. Middle Triassic paleomagnetic data from northern Bulgaria: constraints on Tethyan magnetostratigraphy and paleogeography. Palaeogeogr. Palaeoclimatol. Palaeoecol. 160, 223–237.

Nakov, R., 2001. Late Miocene to Recent Sedimentary Basins of Bulgaria. Geological Society of America, Boulder CO. 28 p.

Panaiotu, C., 1998. Paleomagnetic constrains on the geodynamic history of Romania. In: Ioane, D. (Ed.), Monograph of Southern Carpathians. Reports on Geodesy, vol. 7, pp. 205–216.

Panaiotu, C., 1999, Paleomagnetic studies in Romania: tectonophysic implications. (PhD thesis in Romanian): Bucharest, University of Bucharest.

Patrascu, S., Panaiotu, C., Seclaman, M., Panaiotu, C.E., 1994. Timing of rotational motion of Apuseni Mountains (Romania): paleomagnetic data from Tertiary magmatic rocks. Tectonophysics 233, 163–176.

Pecskay, Z., Harkovska, A., Hadjiev, A., 2000. K–Ar dating of Mesta volcanics (SW Bulgaria). Geol. Balc. 30, 3–12.

Ricou, L.-E., Burg, J.-P., Godfriaux, I., Ivanov, Z., 1998. Rhodope and Vardar: the metamorphic and the olistostromic paired belts related to the Cretaceous subduction under Europe. Geodyn. Acta 11, 285–309.

Ring, U., Layer, P.W., Reischmann, T., 2001. Miocene high-pressure metamorphism in the Cyclades and Crete, Aegean Sea, Greece: evidence for large-magnitude displacement on the Cretan detachment. Geology 29, 395–398.

Schettino, A., Scotese, C.R., 2005. Apparent polar wander paths for the major continents (200 Ma to the present day): a palaeomagnetic reference frame for global tectonic reconstructions. Geophys. J. Int. 163, 727–759.

Schmid, S.M., Berza, T., Diaconescu, V., Froitzheim, N., Fügenschuh, B., 1998. Orogen-parallel extension in the Southern Carpathians. Tectonophysics 297, 209–228.

Schmid, S.M., Bernoulli, D., Fügenschuh, B., Matenco, L., Schefer, S., Schuster, R., Tischler, M., Ustaszewski, K., 2008. The Alps–Carpathians–Dinarides connection: a compilation of tectonic units. Swiss J. Geosci. 101.

Sinclair, H.D., Juranov, S.G., Georgiev, G., Byrne, P., Mountney, N.P., 1997. The Balkan thrust wedge and foreland basin of eastern Bulgaria: Structural and stratigraphic development. In: Robinson, A.G. (Ed.), Regional and Petroleum Geology of the Black Sea and Surrounding Region. AAPG Memoir, vol. 68, pp. 91–114.

Sokoutis, D., Brun, J.-P., van den Driessche, J., Pavlides, S., 1993. A major Oligo-Miocene detachment in southern Rhodope controlling north Aegean extension. J. Geol. Soc. Lond. 150, 243–246.

Speranza, F., Islami, I., Kissel, C., Hyseni, A., 1995. Palaeomagnetic evidence for Cenozoic clockwise rotation of the external Albanides. Earth Planet. Sci. Lett. 129, 121–134.

Sperner, B., Ratschbacher, L., Nemcok, M., 2002. Interplay between subduction retreat and lateral extrusion: tectonics of the Western Carpathians. Tectonics 21. doi:10.1029/2001TC901028.

Tari, G., Dicea, O., Faulkerson, J., Georgiev, G., Popv, S., Stefanescu, M., Weir, G., 1997. Cimmerian and Alpine stratigraphy and structural evolution of the Moesian Platform (Romania/Bulgaria). In: Robinson, A.G. (Ed.), Regional and Petroleum Geology of the Black Sea and Surrounding Region. AAPG Memoir, vol. 68, pp. 63–90.

Tauxe, L., 1998. Paleomagnetic Principles and Practice. Kluwer Academic Publisher, Dordrecht. 299 p.

Torsvik, T.H., Dietmar Müller R., Van der Voo, R., Steinberger, B., Gaina, C. in press. Global plate motion frames: toward a unified model. Rev. Geophys. doi:10.1029/2007RG000227.

Tzankov, T.Z., Angelova, D., Nakov, R., Burchfiel, B.C., Royden, L.H., 1996. The Sub-Balkan graben system of central Bulgaria. Basin Res. 8, 125–142.

Ustaszewski, K., Schmid, S.M., Fügenschuh, B., Tischler, M., Kissling, E., Spakman, W., in press. A map-view restoration of the Alpine-Carpathian-Dinaridic system for the Early Miocene. Swiss Journal of Geosciences (v).

van Hinsbergen, D.J.J., Hafkenscheid, E., Spakman, W., Meulenkamp, J.E., Wortel, M.J.R., 2005a. Nappe stacking resulting from subduction of oceanic and continental lithosphere below Greece. Geology 33, 325–328.

van Hinsbergen, D.J.J., Langereis, C.G., Meulenkamp, J.E., 2005b. Revision of the timing, magnitude and distribution of Neogene rotations in the western Aegean region. Tectonophysics 396, 1–34.

van Hinsbergen, D.J.J., Zachariasse, W.J., Wortel, M.J.R., Meulenkamp, J.E., 2005c. Underthrusting and exhumation: a comparison between the External Hellenides and the “hot” Cycladic and “cold” South Aegean core complexes (Greece). Tectonics 24, TC2011 doi:10.1029/2004TC001692.

van Hinsbergen, D.J.J., van der Meer, D.G., Zachariasse, W.J., Meulenkamp, J.E., 2006. Deformation of western Greece during Neogene clockwise rotation and collision with Apulia. Int. J. Earth Sci. 95, 463–490.

Vandamme, D., 1994. A new method to determine paleosecular variation. Phys Earth Planet. Inter. 85, 131–142.

Vasiliev, I., Krijgsman, W., Stoica, M., Langereis, C.G., 2005. Mio-Pliocene magnetostratigraphy in the southern Carpathian foredeep and Mediterranean–Paratethys correlations. Terra Nova 17, 376–384.

Wortel, M.J.R., Spakman, W., 2000. Subduction and slab detachment in the Mediterranean–Carpathian region. Science 290, 1910–1917.

Yanev, Y., Pecskay, Z., 1997. Preliminary data on the petrology and K–Ar dating of the Oligocene volcano Briastovo, Eastern Rhodopes. Geochim. Miner. Petrol. 32, 59–66.

Yanev, Y., Pecskay, Z., Lilov, P., 1993. K–Ar age and geodynamic position of basic volcanics of the Moesian platform. Rev. Bulg. Geol. Soc. 54, 71–77.

Yanev, Y., Innocenti, F., Manetti, P., Serri, G., 1998. Upper Eocene–Oligocene collision-related volcanism in Eastern Rhodopes (Bulgaria)—Western Thrace (Greece): petrogenic affinity and geodynamic significance. Acta Volcanol. 10, 279–291.

Zhao, X., Riisager, P., Antretter, M., Carlut, J., Lippert, P., Liu, Q., Galbrun, B., Hall, S., Delius, H., Kanamatsu, T., 2006. Unraveling the magnetic carriers of igneous cores from the Atlantic, Pacific, and the southern Indian oceans with rock magnetic characterization. Phys. Earth Planet. Inter. 156, 294–328.

Zijderveld, J.D.A., 1967. A.c. demagnetisation of rocks: analysis of results. In: Collinson, D.W., et al. (Ed.), Methods in Palaeomagnetism. Amsterdam, Elsevier, pp. 254–286.

Zweigel, P., Ratschbacher, L., Frisch, W., 1998. Kinematics of an arcuate fold-thrust belt: the southern Eastern Carpathians (Romania). Tectonophysics 297, 177–207.

Please cite this article as: van Hinsbergen, D.J.J., et al., No significant post-Eocene rotation of the Moesian Platform and Rhodope (Bulgaria): Implications for the kinematic evolution of the Carpathian and Aegean arcs, Earth Planet. Sci. Lett. (2008), doi:10.1016/j.epsl.2008.06.051